ILLINOIS

UNIVERSITY OF ILLINOIS AT URBANA-CHAMPAIGN

-

PRODUCTION NOTE

University of Illinois at
Urbana-Champaign Library
Large-scale Digitization Project, 2007.

UNIVERSITY OF ILLINOIS BULLETIN

Vol. V. SEPTEMBER 2, 1907 No. 1

[Entered Feb. 14, 1902, at Urbana, Illinois, as second-class matter under Act of Congress July 16, 1894]

BULLETIN NO. 18 - 36

1907-09

THE STRENGTH OF CHAIN LINKS

BY

G. A. GOODENOUGH

AND

L. E. MOORE

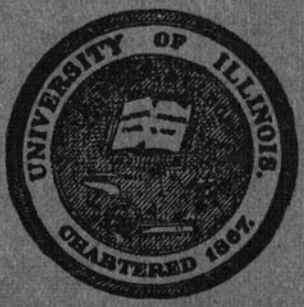

UNIVERSITY OF ILLINOIS
ENGINEERING EXPERIMENT STATION

URBANA, ILLINOIS

PUBLISHED BY THE UNIVERSITY

THE Engineering Experiment Station was established by action of the Board of Trustees December 8, 1903. It is the purpose of the Station to carry on investigations along various lines of engineering, and to study problems of importance to professional engineers and to the manufacturing, railway, mining, constructional and industrial interests of the state.

The control of the Engineering Experiment Station is vested in the heads of the several departments of the College of Engineering. These constitute the Station Staff, and with the Director determine the character of the investigations to be undertaken. The work is carried on under the supervision of the Staff; sometimes by a research fellow as graduate work, sometimes by a member of the instructional force of the College of Engineering, but more frequently by an investigator belonging to the Station corps.

The results of these investigations will be published in the form of bulletins, and will record mostly the experiments of the Station's own staff of investigators. There will also be issued from time to time in the form of circulars, compilations giving the results of the experiments of engineers, industrial works, technical institutions and governmental testing departments.

The volume and number at the top of the title page of the cover are merely arbitrary numbers and refer to the general publications of the University of Illinois; *above the title is given the number of the Engineering Experiment Station bulletin or circular, which should be used in referring to these publications.*

For copies of bulletins, circulars or other information, address the Engineering Experiment Station, Urbana, Illinois.

Issued March, 1908

UNIVERSITY OF ILLINOIS BULLETIN

Vol. V. SEPTEMBER 2, 1907 No. 1

[Entered Feb. 14, 1902, at Urbana, Illinois, as second-class matter under Act of Congress July 16, 1894]

BULLETIN NO. 18

THE STRENGTH OF CHAIN LINKS

BY

G. A. GOODENOUGH

AND

L. E. MOORE

UNIVERSITY OF ILLINOIS
ENGINEERING EXPERIMENT STATION

URBANA, ILLINOIS

PUBLISHED BY THE UNIVERSITY

This page is intentionally blank.

UNIVERSITY OF ILLINOIS
ENGINEERING EXPERIMENT STATION

BULLETIN NO. 18 SEPTEMBER 1907

THE STRENGTH OF CHAIN LINKS

By G. A. Goodenough[1], *Associate Professor of Mechanical Engineering, University of Illinois and L. E. Moore, Assistant Professor of Civil Engineering, Massachusetts Institute of Technology, formerly Associate in Theoretical and Applied Mechanics, University of Illinois.*

The chain is one of the most familiar as well as one of the most useful of mechanical devices. It is universally employed in hoisting and transmission, and for attaching and securing movable bodies, as, for example, in anchoring ships. As a rule, a chain is subjected to heavy loads and must transmit large forces, and upon its ability to withstand the stresses to which it is subjected by its loading may depend the success of a great mechanical operation, or even the safety of lives.

In view of these facts, it is surprising that the chain has received scant attention from investigators in the field of elasticity and strength of materials. Aside from two or three scattered memoirs, the theory of the stresses in chain links has been untouched. Experiments have been made, it is true, but these have been for the purpose of determining the ultimate strength of the chain, not for the purpose of testing a theory. Formulas for the loading of chains have been based upon the ultimate strength of the chain when tested to destruction and are thus purely empirical. No attempt seems to have been made to place such formulas on a rational basis supported by theory. It may be urged that the present empirical rules are satisfactory, inasmuch as they lead to satisfactory results. As a matter of fact, the results are not satisfactory; chains break, often with disastrous consequences, and the only reason that more do not

[1] For the theoretical analyses contained in the appendices and for the discussion of the experimental results Professor Goodenough is responsible. The experimental work was conducted under the direction and supervision of Professor Moore, and he is responsible for the methods employed in making the tests and for the accuracy of the experimental results.

break is that a chain is seldom subjected to its rated load. Further arguments to show the importance of a rational analysis seem hardly necessary.

In undertaking the work described in this paper, three things were held in view.

(1) The development of the theory of the stresses induced in chain links with given conditions as regards loading.

(2) Experimental tests of the validity of the theory employed and also of the validity of the assumptions made as to the distribution of pressure between adjacent links.

(3) The deduction from theoretical considerations alone of rational formulas for the loading of chains.

The beginning of this work dates back to 1900, when the analytical investigations were largely worked out. In 1906, Mr. R. M. Evans of the class of 1906 undertook the experimental verification of the theory, and presented in his graduating thesis certain of the results contained herein. The following year the experimental work was continued by Messrs. M. L. Millspaugh and R. L. Baker. The data obtained have been worked over carefully, all calculations have been repeatedly checked, and it is believed that the results derived are worthy of confidence, whatever may be the conclusions that are drawn from them.

Method of Analysis

The analytical investigation was first suggested by Bach's analysis of the stresses in a hollow cylindrical roller.[1] It seemed evident that the general method there used could be employed to determine the stresses in links with circular or elliptical center lines. The fundamental equations may be found in Bach's work, but for the sake of completeness they are given in condensed form in this paper. (See Appendix A.) Grashof[2] gives an analysis using the same fundamental equations, but owing to untenable assumptions, the analysis gives results wide of the truth. The only other analysis is that made by Winkler in a memoir published in Der Civilingenieur.[3] A

[1] Bach, *Elasticitat und Festigkeit*, p. 458.

[2] Grashof, *Elasticitat und Festigkeit*, Sec. 178–180, pp. 273–277.

[3] *Formandering und Festigkeit Gekrummter Körper in besondere der ringe.* Der Civilingenieur, Bd. IV; S. 232–246.

discussion of this memoir in which some of the results have been corrected is given by Professor Karl Pearson.[1] To show Pearson's estimate of Winkler's work the following paragraphs from the introduction of the discussion are quoted:

"This is an important memoir both from the theoretical and practical standpoint; although many of its results require correction and modification. Some of these corrections have been made in Kapitel XL (*Ringformige Körper*) of the author's well known treatise: *Die Lehre von der Elasticität und Festigkeit*, Prag, 1867, but this treatise does not cover anything like the same area as the memoir. I propose therefore to indicate the correct analysis and compare its results with those of Winkler.

"The importance of the subject will be sufficiently grasped when I remind the reader that it is the only existing theory of the strength of the links of chains. To investigate the strength of such links by the complete theory of elasticity would involve even for the case of anchor rings an appalling investigation in toroidal and allied functions; while for the oval chain links with studs in ordinary use, any successful attempt at a general investigation seems inconceivable. We shall have the less hesitation, however, in applying the Bernoulli-Eulerian theory, if we remember how close an approximation Saint-Venant's researches on flexure have shown it to be in the case of *straight* bars. At the same time we are certainly going to put it to the very limit of its application, namely, to *curved* bars in which the dimensions of the cross sections are not very small as compared with either the length or the radius of curvature of the central axis." . . .

"Remembering that we need not assume adjacent cross sections of our link to remain undistorted, if we only suppose them to be approximately equally distorted, we can easily investigate an expression for the stretch at any point by a method akin to that which results from the Bernoulli-Eulerian theory."

The method here referred to is that given by Bach and Grashof for the analysis of bars with curved axes. An outline of it, as already stated, is given in Appendix A.

While the method employed in the investigations herein described

[1] Todhunter and Pearson, *History of the Elasticity and Strength of Materials.* Vol. II, Part I, p. 423 et seq.

is essentially the same as that of Winkler and Pearson, there are one or two important points of difference in the assumptions made. Professor Pearson considers only two cases, the link with elliptical center line, and the link made up of two circular arcs and two straight lines. The analysis here given is extended to links of four and six circular arcs so as to approximate as closely as possible to the forms actually occurring; it is also extended to links with studs. Furthermore, it appears that in all cases Winkler assumed the pressure between adjacent links to be concentrated at a point at the end of the link. The present analysis assumes a distribution of pressure over a definite area. As will be shown later, this question of distribution has an important bearing upon the results obtained.

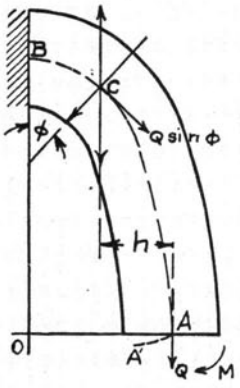

FIG. 1.

The complete analysis of the open link is given in Appendix B. The following is merely a brief outline of the method of attacking the problem. Consider one quadrant of the link as shown in Fig. 1. Denoting by $2Q$ the load on the link, the section at A lying along the minor axis will be subjected to a normal force Q. There will also be at this section a bending moment M, which can be determined from the conditions of the problem. Now assume any other normal section, as C, and consider the part of the link between sections A and C a free body. At C let two forces, each equal to Q but opposite in sense, be added to the system. One of these forces with the force Q at section A forms a couple whose moment is Qh; the other force is resolved into components, one $Q \cos \phi$ along the section, the other $Q \sin \phi$ normal to the section. The component $Q \cos \phi$ produces shearing stress and is neglected in the subsequent discussion. At the section C we have therefore:

$$\text{a normal force, } P = Q \sin \phi;$$
$$\text{a bending moment, } M_b = Qh + M.$$

The unknown moment M is now found from considerations explained in the analysis; and with P and M_b fully known, the intensity

of stress at any fiber is readily determined from the fundamental equation (C), Appendix A. It may be noted that instead of (C), the usual formula

$$S = \frac{P}{f} + \frac{M_y}{I}.$$

may be used, though the results may not be quite exact.

Pressure Between Adjacent Links

At the very beginning of the analysis arises a question as to the way in which the pressure between adjacent links is distributed. The analysis is somewhat simplified by assuming that two links have contact at one point only and that in consequence the pressure between them is concentrated at this point. [See Fig. 2(a)]. As a matter of fact, however, the links after a little wear have contact over a con-

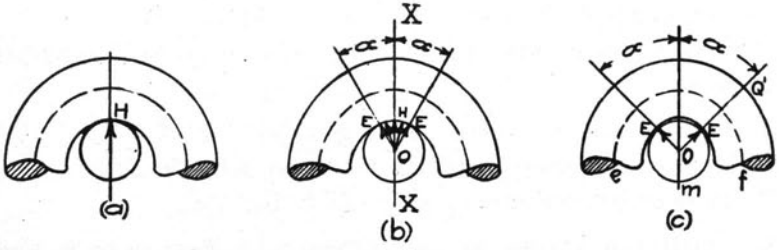

Fig. 2.

siderable surface and the pressure between them must be distributed in some way or other over this surface.

Referring to Fig. 2(b), suppose that contact exists over the arc EE, which subtends the angle 2α at the center O. Though the parts of the link in contact are curved, the action of one link on another may be likened to that of a journal and bearing. We may assume (1) that the pressure is uniformly distributed along the arc EE, or if we make use of the more exact analysis of journal and bearing, we may assume (2) that the intensity is greatest at H and decreases towards E, being at any point proportional to the cosine of the angle made with the axis XX. Because angle α is small, the second assumption changes but little the results obtained by using

the first; hence we shall consider only the assumption of uniform distribution.

A third possible distribution is represented in Fig. 2(c). Under heavy load the link suffers a considerable distortion and the sides e and f approach each other. Now if the distributed pressure along EE, Fig. 2(b), were in the nature of a fluid pressure so that the points of application of the forces could move as the points EE moved, the law of distribution would be unchanged by the distortion of the link. But the part m of the adjacent link lying between the sides e and f is practically unyielding; hence when e and f approach each other the part m is pinched and there ensues a new distribution of pressure. Evidently the result of this pinching action is to increase the intensity of pressure near E, E and to decrease it at H. We cannot, of course, know the precise effect of the action just described. For the sake of comparison with the other cases, we may assume, however, that the effect is equivalent to concentrating the pressure at the two points E, E.

In the subsequent analysis we shall make the three assumptions just stated, namely:

(1) Pressure concentrated at single point H, Fig. 2(a).
(2) Pressure uniformly distributed over arc EE, Fig. 2(b).
(3) Pressure concentrated at points E, E, Fig. 2(c).

As a matter of interest, we may in passing call attention to Grashof's analysis. The links are supposed to be in contact along an arc EE subtending the angle 2α, as in Fig. 2(c). It is then assumed that the part of the link lying between the sections E, E takes no part in the straining action, but acts as a rigid base or foundation to which are attached the sides e and f. As will be shown later, this neglected part of the link plays a most important rôle, and Grashof's assumption is anything but justified.

Experimental Verification of Analysis

Referring to Fig. 1, OA and OB denote respectively the semi-minor and semi-major axes of the link. Under a load these axes change, OA becomes shorter and OB longer, and these changes can be measured with reasonable accuracy. Now the theoretical analysis

here employed furnishes a means of calculating the change of position of any point, as, for example, the point A, on the center line of the link. Thus for a given load, the new position A' to which A will move can be found. Evidently the component of AA' in the direction of AO is the change in OA, that is, one-half the change in the length of the minor axis; likewise, the component of AA' in the direction of OB is one-half the change in the major axis.

We have here a means of verifying theory by experiment. The changes of length of the axes of the link for given loads can be cal-

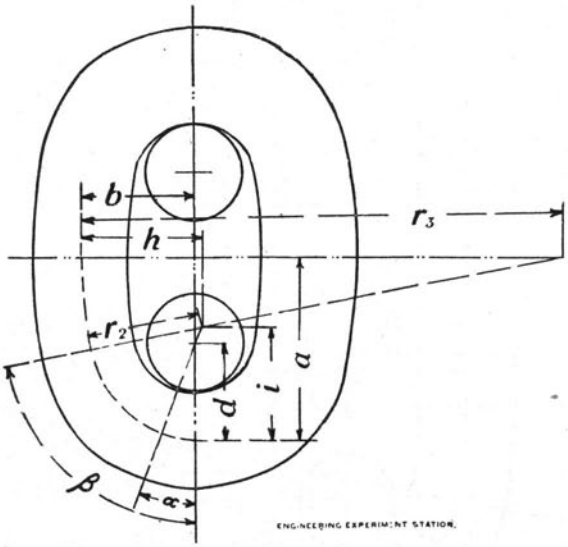

FIG. 3.—DREDGE CHAIN.

Dimensions.

$d=1.000$ in.	$b=1.178$ in.	$i=1.161$ in.	$r_2=1.173$ in.	$\alpha=21°$
$a=1.875$ in.	$h=1.240$ in.	$e=0.000$ in.	$r_3=5.000$ in.	$\beta=79°15'$

culated from purely theoretical considerations. The actual changes for those loads can be measured. A comparison of the calculated and actual values of the changes of length affords therefore a delicate test of the theoretical analysis.

Because of the doubt regarding the distribution of pressure between adjacent links it was considered advisable to use circular rings of rectangular cross section. With these rings a true knife-edge bearing was possible, and the general theory (Appendix A) could be tested without danger of introducing unknown factors resulting from the

pressure distribution. The experiments on the rings are to be considered, therefore, as more reliable than the link tests in establishing the truth or falsity of the analysis. The tests of the actual chain links are, however, valuable in two ways: (1) They may be used to

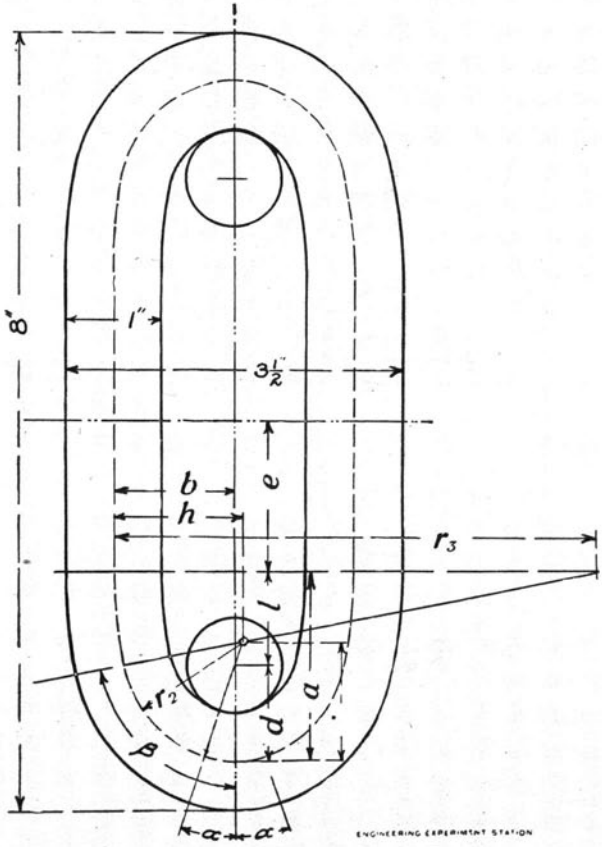

FIG. 4. — CONVEYOR CHAIN.

Dimensions.

$d = 1.00$ in.	$b = 1.23$ in.	$i = 1.294$ in.	$r_2 = 1.340$ in.	$\alpha = 30°0'$
$a = 2.00$ in.	$h = 1.40$ in.	$e = 1.500$ in.	$r_3 = 5.000$ in.	$\beta = 78°53'$

establish more firmly the analysis when applied to oval links; (2) Assuming that the ring experiments sufficiently establish the analysis, the link experiments may be used to test the assumptions made as to the distribution between adjacent links.

As already stated, the experiments were extended over a period of

two years and were performed as thesis work in the Laboratory of Applied Mechanics of the University of Illinois by senior students in the College of Engineering. The experiments of the first year (1906) made by R. M. Evans were wholly on chain links. Those of the second year (1907) made by Messrs. Baker and Millspaugh were partly on heavy chain links and partly on finished steel rings. These three men deserve great credit for the amount and the character of

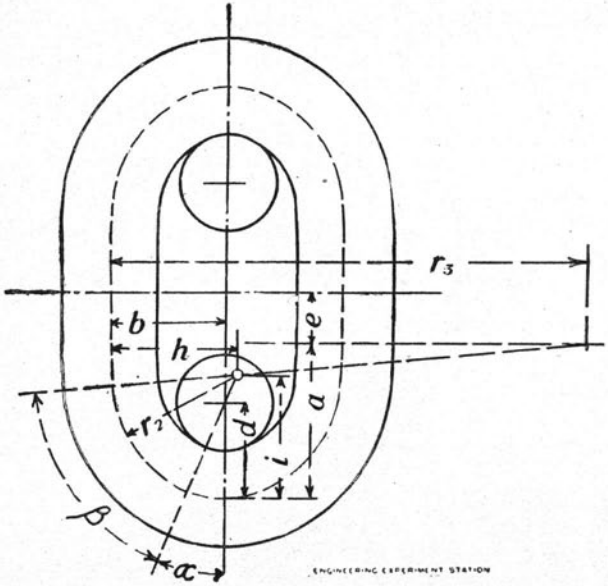

FIG. 5. — PROOF COIL CHAIN.

Dimensions.

d=1.00 in.	b=1.214 in.	i=1.316 in.	r_2=1.35 in.	α=25°18⅔′
a=1.625 in.	h=1.364 in.	e=0.500 in.	r_3=5.00 in.	β=85°9′

the work done and for their untiring efforts to do the work as well and accurately as possible.

It has not seemed necessary or desirable to differentiate in these pages between the tests made in the different years, as the objects of the tests and methods used were the same. The chain links tested were ordinary commercial links bought in the market. The test pieces for determining the modulus of elasticity of the material were ordered cut from the same bar from which the chains were made. The links with dimensions are shown in Fig. 3, 4, 5 and 6. In making the tests a short piece of chain, consisting of either three or five links,

five links being used whenever the dimensions of the machine would permit, was held in the jaws of the testing machine by a clevis at each end. These clevises were flattened to afford a better grip for the jaws of the machine. This is illustrated in Fig. 7. Deformations

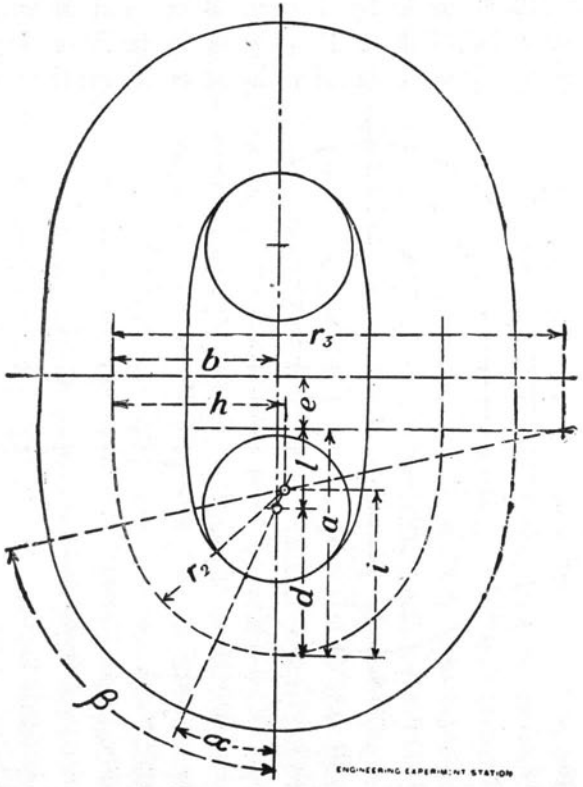

FIG. 6. — TWO-INCH DREDGE CHAIN.

Dimensions.

$d=2$ in.	$b=2.214$ in.	$i=2.305$ in.	$r_2=2.333$ in.	$\alpha=24°0'$
$a=3.125$ in.	$h=2.42$ in.	$e=0.7$ in.	$r_3=6.25$ in.	$\beta=77°54\frac{1}{3}'$

were measured by micrometers reading directly to .001 inch, and by interpolation to .0001 inch.

A micrometer having a "rachet contact" which insured practically the same pressure on the points in all measurements was used for measuring the deformations of the transverse or minor axis. To insure measuring between the same points each time small brass buttons were soldered to all the links except the 2-in. dredge chain

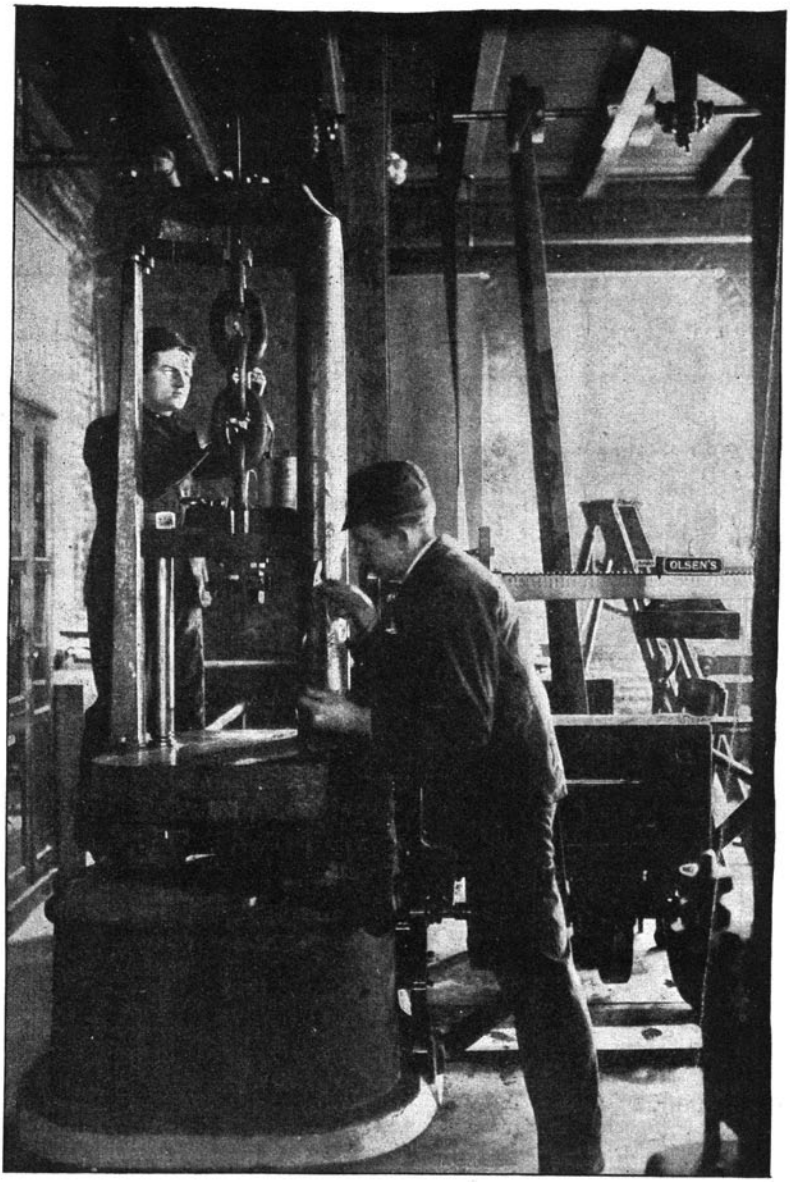

FIG. 7.

link at the ends of the minor axis. The measurements were taken over these buttons. On the dredge chain a small spot was polished on the link itself at each end of the axis. The longitudinal deformations were taken between brass contact points screwed to the inside of two transverse bars of $\frac{3}{4}$-in. square iron. One of these bars was soldered to the link at each end of the long diameter or major axis. The distance between the contact points was then readily measured by means of an inside micrometer. An electric bell and battery were used in this connection, the bell ringing as soon as contact was established between the points. This device is shown in Fig. 8 and 9.

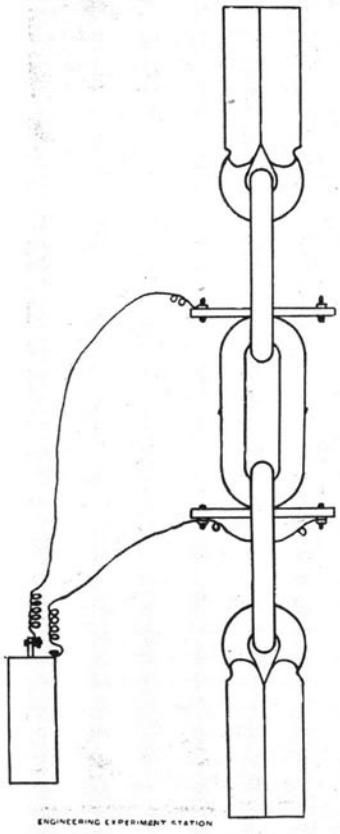

FIG. 8.

The dimensions of the rings were 12 in. outside and 9 in. inside diameter by 1 in. thick, as shown in Fig. 10. Two of these rings were cast steel and the third was wrought steel with a perfect weld. The rings were finished all over in a lathe. The method of holding the rings in the machine and applying the load is clearly shown in Fig. 11 and 12. The load was applied to the ring through knife edges. This was done to remove the uncertainty as to the distribution of pressure between the links. By referring to Fig. 11 and 12 it will be noted that the method of loading the rings gives flexibility in all directions and prevents any eccentricity of loading.

The moduli of elasticity of the different materials were determined from test specimens cut, except in the case of the cast steel rings, from the same bars from which the chains and ring were made. The modulus of elasticity of the cast steel was determined from test pieces poured from the same heat as the rings.

The plan followed in testing was to increase the load by such nearly equal increments that from fifteen to twenty readings would have been obtained when the estimated elastic limit was reached. In testing the links the load was increased to a point just beyond the elastic limit, which was indicated by the change in the increment of the deformation. The links were allowed to rest at least twenty-four hours and the second test was then run up to the same maximum load as in the first case, no attention being paid to the possible raising of

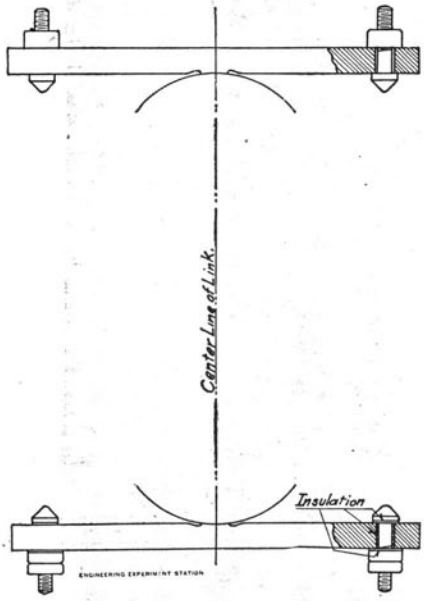

FIG. 9.

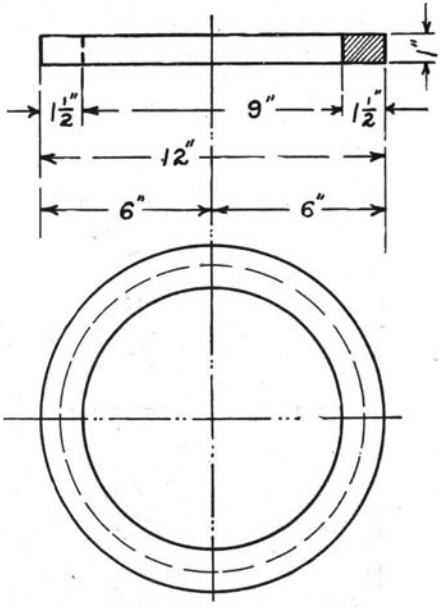

FIG. 10.

the elastic limit by this treatment. It may be readily seen that the exact elastic limit is of little importance in this work compared to the modulus of elasticity. So long as the material was not injured to such an extent as to render values of the modulus of elasticity doubtful, the slight exceeding of the elastic limit was of no consequence. In testing the rings care was taken not to exceed the elastic limit.

In all cases save one, two tests of each specimen will be found recorded, and called the "first test" and the "second test" respec-

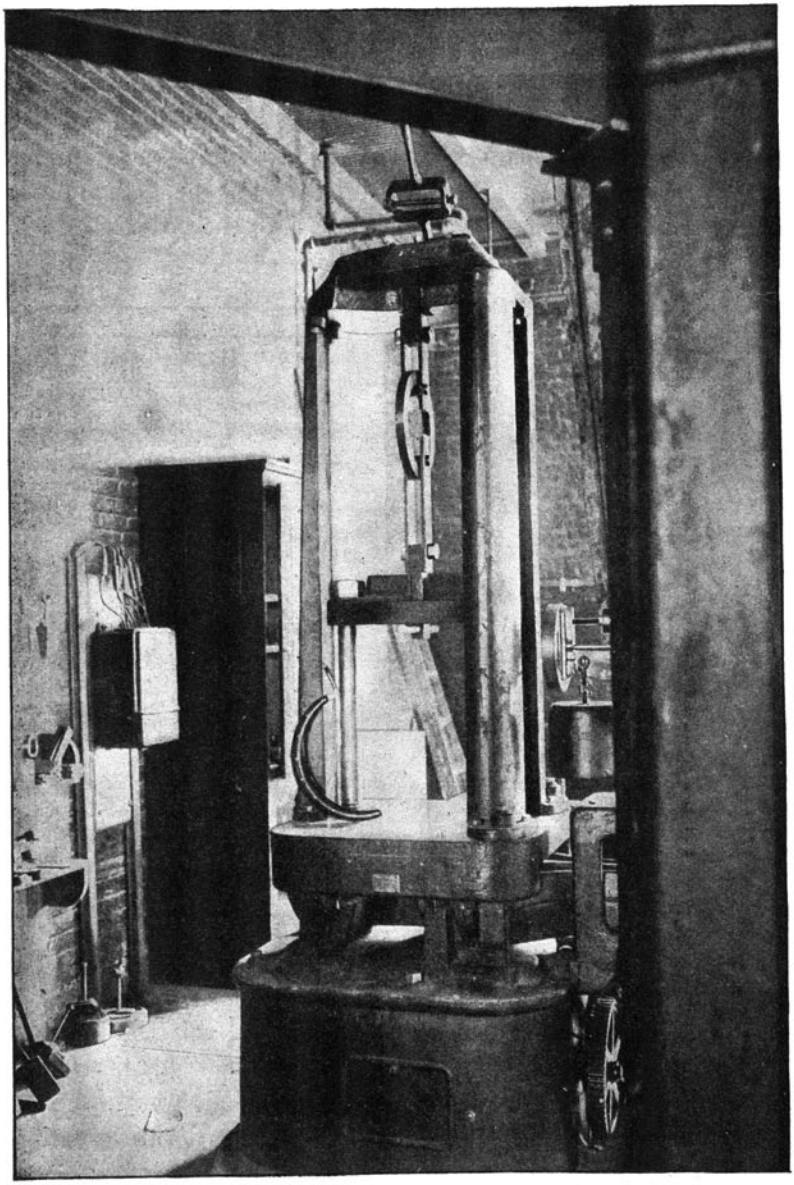

FIG. 11.

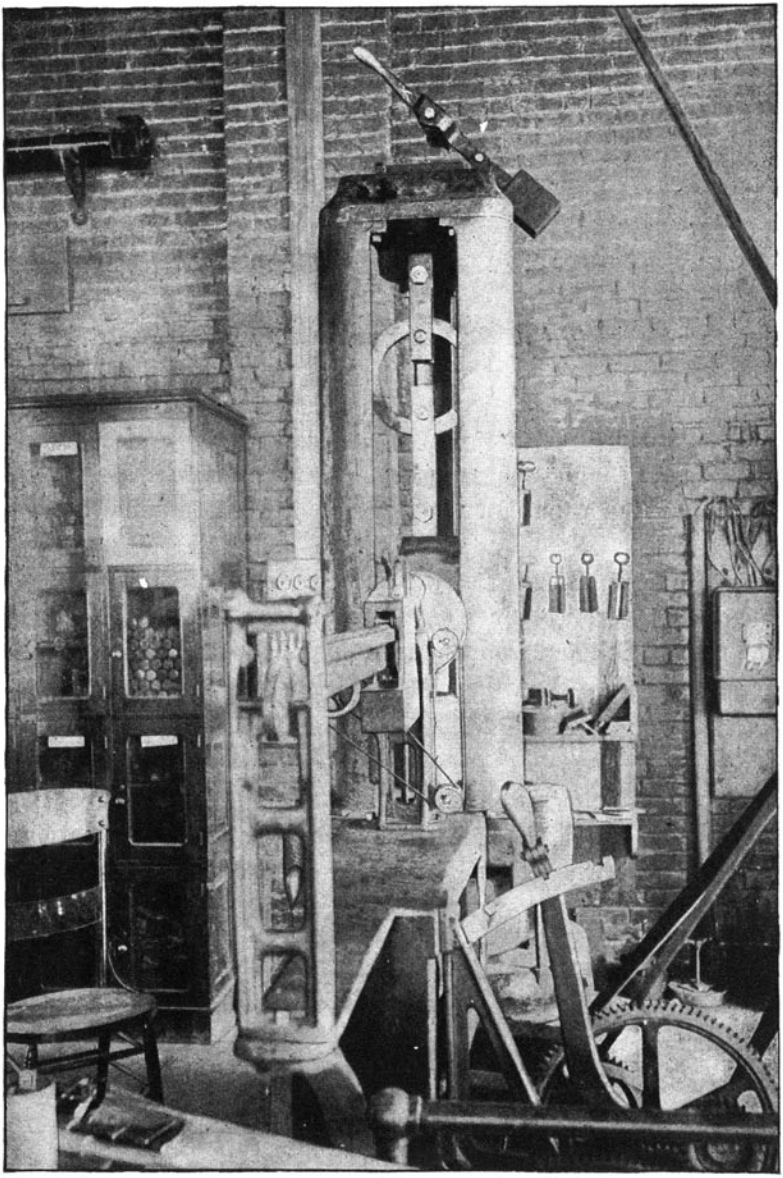

FIG. 12.

tively. These were not the only tests run. In some cases it was found desirable to run one or two preliminary tests to accustom the students to taking their observations and to get an idea of the behavior of the piece under load.

Results

The results of the tests are given in tabular form on pages 37-44. Tables 6 to 11 inclusive apply to the tests of the circular rings; tables 12 to 18 to the tests of the four chain links shown in Fig. 3, 4, 5 and 6. The headings of the various columns render detailed explanation of the tables unnecessary.

The tabular values plotted to scale are shown in Fig. 13 to 25 inclusive. Fig. 13 to 18 show the results obtained from the circular rings; Fig. 19 to 25 those from the chain links. The first test in each case is denoted by a small circle o, the second test by a filled circle, ●. For the sake of convenience in comparison, the two tests are given in the same figure, but for distinctness, different origins have been used.

It is to be emphasized that the lines appearing in these figures are in all cases theoretical lines calculated from the known dimensions of the ring or link and from the modulus of elasticity experimentally determined. These lines in fact could have been drawn before the deflection tests were made.

Discussion of Experimental Results

1. *Circular Rings.* Table 1 gives the calculated deformation for the three circular rings tested.

TABLE 1

DEFLECTION OF CIRCULAR RINGS

	Change of Length of Diameter per 1000-lb. Load	
	Vertical Diameter Inches	Horizontal Diameter Inches
No. 1	.00286	.00247
No. 2	.00294	.00254
No. 3	.00263	.00228

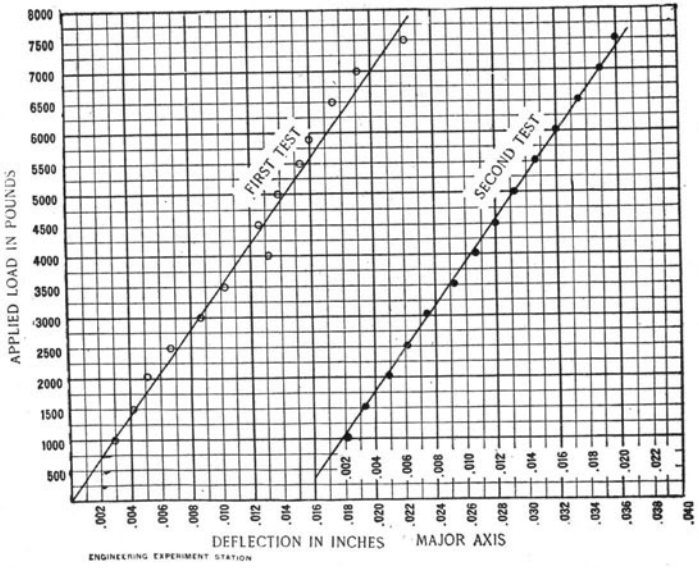
APPLIED LOAD IN POUNDS
8000
7500
7000
6500
6000
5500
5000
4500
4000
3500
3000
2500
2000
1500
1000
500
FIRST TEST
SECOND TEST
DEFLECTION IN INCHES MAJOR AXIS
ENGINEERING EXPERIMENT STATION

FIG. 13.

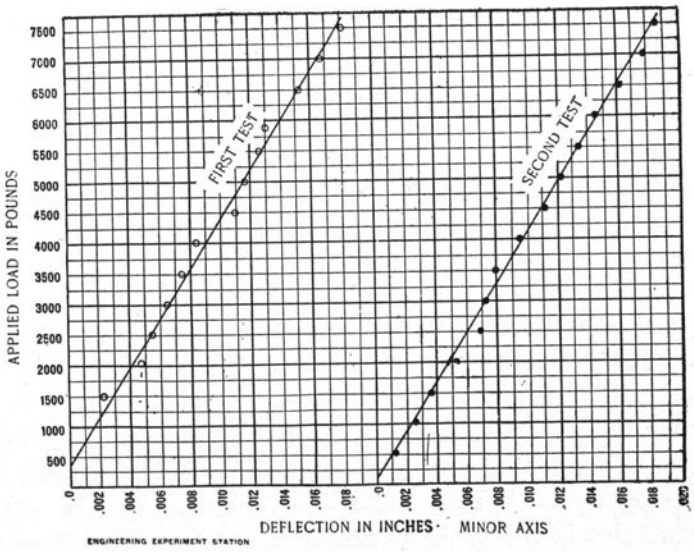
APPLIED LOAD IN POUNDS
7500
7000
6500
6000
5500
5000
4500
4000
3500
3000
2500
2000
1500
1000
500
FIRST TEST
SECOND TEST
DEFLECTION IN INCHES · MINOR AXIS
ENGINEERING EXPERIMENT STATION

FIG. 14.

The values in this table were obtained from equations (H′) Appendix C. The following is the calculation for ring No. 1:

$$\text{Mean radius } r = 5.25 \text{ in.}$$

$$\text{Area of cross section } f = 1.5605 \text{ sq. in.}$$

Modulus of elasticity (by experiment), 26,200,000.

$z = .006887$; (See Appendix A).

$$\frac{1}{z} = 145.197;$$

$$\frac{1}{1+z} = .99315$$

Substituting in formulas (H′), p. 65,

$$\Delta x_a = -\left[\frac{5.25 \times 145.197}{26{,}200{,}000 \times 1.5605}\left(\frac{2 \times .99315}{3.1416} - 0.7854\right)\right] Q = .00000286 Q,$$

$$\Delta y_a = -\left[\frac{5.25 \times 145.197}{26{,}200{,}000 \times 1.5605}\left(\frac{2 \times .99315}{3.1416} - 0.5\right)\right] Q = -.00000247\, Q.$$

As is evident from (H′), the curve giving the relation between the change of length of the axis and the applied load is a straight line through the origin. The value in the table gives the slope of this line. In Fig. 13 to 18 these lines have been drawn through the plotted points, and a comparison may be made between the line determined by calculation based on analysis and the points found by experiment.

The lines representing the mean of the experimental values will not, in general, pass through the origin, because of unavoidable errors at the beginning of the test. Hence the theoretical lines are not drawn through the origin, but are drawn with the proper slope in such a position as to permit the comparison to be made most easily. This course is entirely justified by the fact that the slope of the line, rather than its absolute position, is the important factor.

In ring No. 1, it will be seen that the agreement is remarkable; in fact, the calculated line is about as near the mean line of the points as could be drawn. It will be noticed that the points of the second test lie a little more regular in all cases than those of the first test.

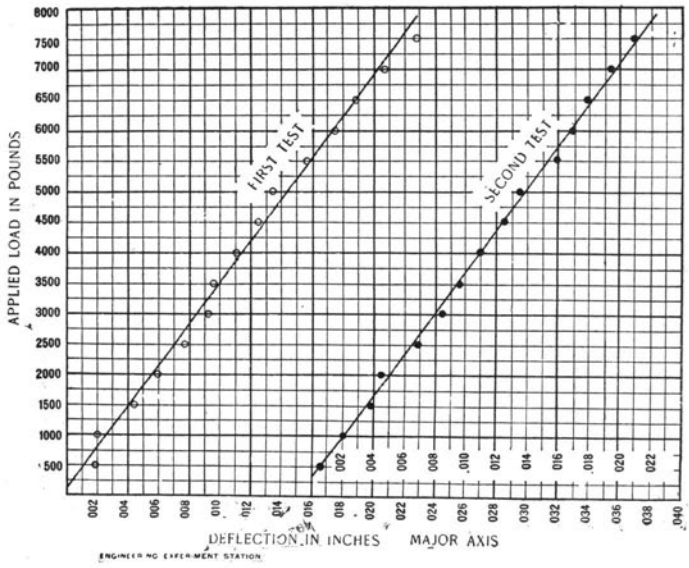
APPLIED LOAD IN POUNDS
FIRST TEST
SECOND TEST
DEFLECTION IN INCHES MAJOR AXIS
ENGINEERING EXPERIMENT STATION

FIG. 15.

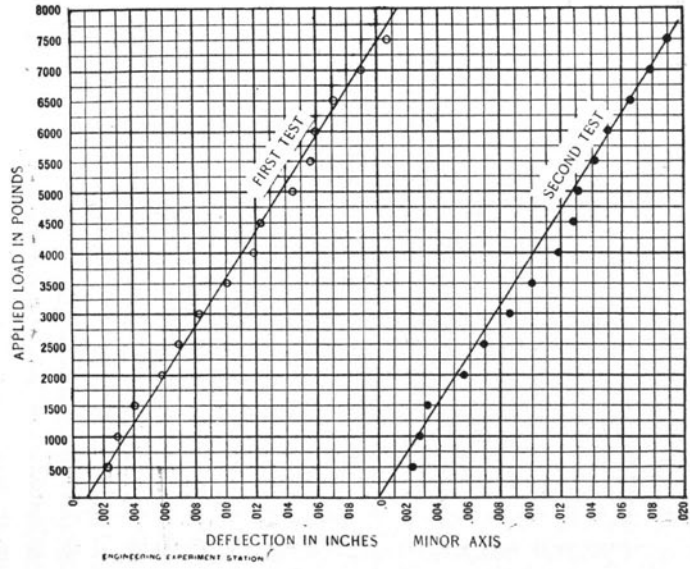
APPLIED LOAD IN POUNDS
FIRST TEST
SECOND TEST
DEFLECTION IN INCHES MINOR AXIS
ENGINEERING EXPERIMENT STATION

FIG. 16.

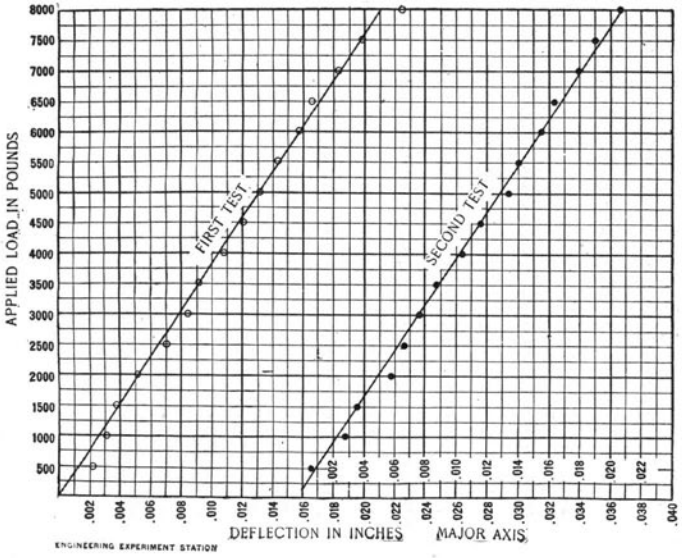
APPLIED LOAD IN POUNDS
8000
7500
7000
6500
6000
5500
5000
4500
4000
3500
3000
2500
2000
1500
1000
500
FIRST TEST
SECOND TEST
.002 .004 .006 .008 .010 .012 .014 .016 .018 .020 .022 .024 .026 .028 .030 .032 .034 .036 .038 .040
DEFLECTION IN INCHES MAJOR AXIS
ENGINEERING EXPERIMENT STATION

FIG. 17.

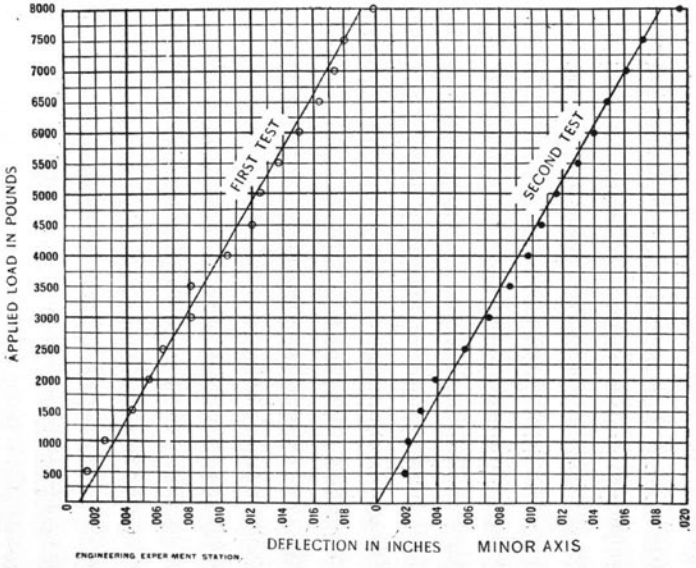
APPLIED LOAD IN POUNDS
8000
7500
7000
6500
6000
5500
5000
4500
4000
3500
3000
2500
2000
1500
1000
500
0
FIRST TEST
SECOND TEST
.002 .004 .006 .008 .010 .012 .014 .016 .018 .020
DEFLECTION IN INCHES MINOR AXIS
ENGINEERING EXPERIMENT STATION

FIG. 18.

In ring No. 2, the agreement is not quite so close as in No. 1, but still is fairly satisfactory. In the case of ring No. 3, vertical axis, the agreement is good, and it is also good in the second test for the

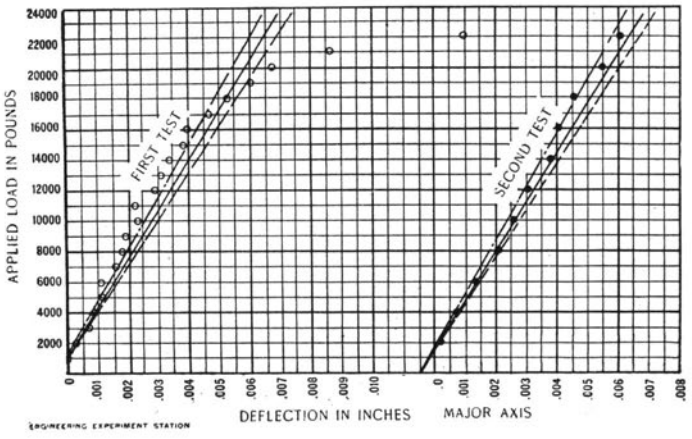

FIG. 19.

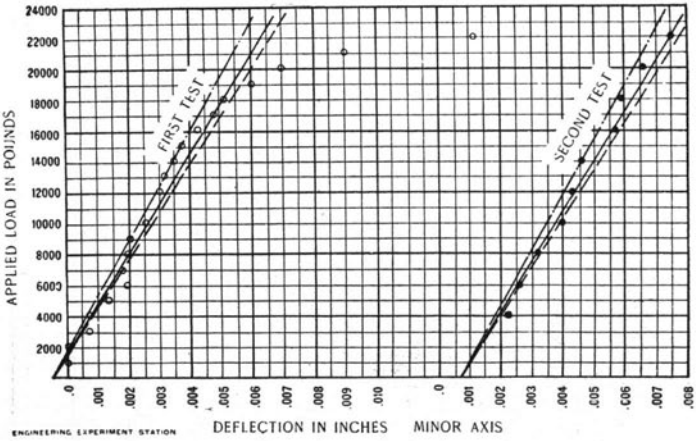

FIG. 20.

horizontal diameter. In the first test the slope of the actual line seems slightly less than that of the calculated lines. It is possible that the modulus of elasticity as determined for rings 1 and 2 is a

little low. A higher value would make the theoretical lines slightly steeper.

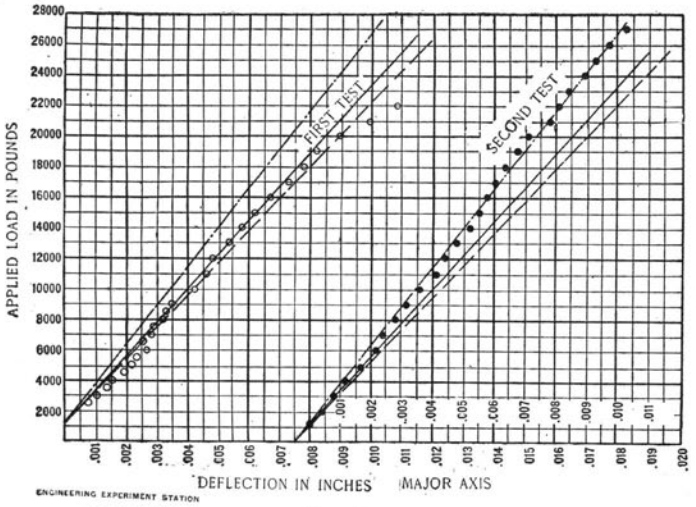

FIG. 21.

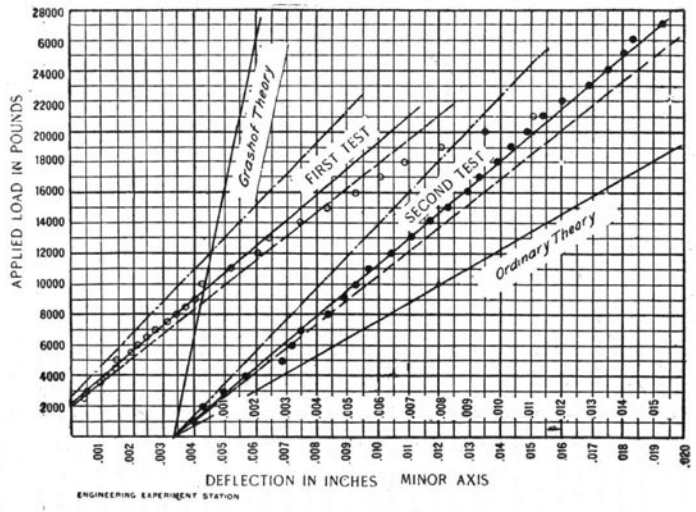

FIG. 22.

The experiments on the rings, on the whole, seem to confirm in a satisfactory manner the theoretical analysis. We may therefore

conclude that the fundamental equations employed will give very closely the true stresses in rings, and that if proper assumptions regarding the distribution of pressure between links be made, the same equations will give the stresses in chain links. Assuming, therefore, the correctness of the analysis, we may use the results of the experiments on the links to throw some light on the question of distribution of pressure.

2. *Chain Links.* Fig. 19 and 20 show the experiments on the link shown in Fig. 3. In this, as in all the chain links, three calculations for the change of length of the axis were made. These correspond to the three assumptions as to the pressure noted in a previous section. See p. 6 and Fig. 2(a), (b), (c). The line of least inclination, indicated thus — — — —, corresponds to case (a), concentration at the end of the link; the intermediate full line corresponds to case (b), distributed pressure; while the line of greatest slope, indicated thus —· —· —· —, corresponds to case (c), concentration at two points due to the possible wedging action. If we direct our attention to the second test, Fig. 19, we observe that the experimental points lie well within the region of these three lines; the same may be said of the test showing the change of length of the minor axis, Fig. 20.

In Fig. 21 and 22 are shown the experiments upon the long link of the conveyor chain, Fig. 4. The coincidence between the points of the second test and the theoretical line, Fig. 22, is striking. This test is perhaps of more weight than any other of the link tests because the length of the link caused large deflections. It will be observed that the points for the first test indicate in each case a line of smaller slope than the points for the second test. This fact may be explained possibly as follows: In the second test the links have become accommodated to each other, so to speak, and the action is more nearly that of a journal and bearing: hence condition (b) is approximated to rather than condition (a).

In Fig. 23 is shown the one test made on the link shown in Fig. 5. For some reason, a second test of this link was not made. The results are about as shown for the other links. Probably the points for the second test would have followed more closely the theoretical lines, as in the other cases.

The experiments upon the two-inch link, Fig. 6, are shown in Fig. 24 and 25. The results of the two tests are practically the same, and the agreement between the experimental points and theoretical lines is satisfactory.

The theoretical lines shown in Fig. 19–25 were obtained by calculation from formulas (J) and (K), Appendix C. The following table gives the results of the calculations thus made: —

TABLE 2

BENDING MOMENTS AND DEFLECTIONS OF CHAIN LINKS

	Case	Dredge Link, Fig. 3 Curves, Fig. 19 and 20	Conveyor Link, Fig. 4 Curves, Fig. 21 and 22	Proof Coil Link, Fig. 6 Curves, Fig. 23	Two-Inch Link, Fig. 6 Curves, Fig. 24 and 25
Bending Moment M at End of Minor Axis	(a)	$-0.353\ Qd$	$-0.233\ Qd$	$-0.329\ Qd$	$-0.326\ Qd$
	(b)	-0.345 "	-0.223 "	-0.318 "	-0.315 "
	(c)	-0.328 "	-0.200 "	-0.294 "	-0.292 "
Increase of Length of Major Axis per 1000 lb. Load.	(a)	0.000324	0.000475	0.000364	0.000144
	(b)	0.000312	0.000449	0.000345	0.000139
	(c)	0.000289	0.000394	0.000312	0.000121
Decrease of Length of Minor Axis per 1000 lb. Load.	(a)	0.000353	0.000628	0.000404	0.000133
	(b)	0.000345	0.000583	0.000384	0.000126
	(c)	0.000328	0.000478	0.000341	0.000111

It is self-evident that the results obtained from the rough chain links would not be as concordant as those obtained from the finished rings. However, a comparison of the experimental values with the theoretical lines, Fig. 19 to 25, indicates that the theory is confirmed fairly well. The links tested exhibited some variety in form and size; and the results of the calculations show that the agreement of theory and experiment was equally good whether the link was long or short, of 1-in. or 2-in. iron. Tests of more links would have been desirable if sufficient time had been available. It may be stated that the computations are somewhat laborious and time-consuming. It is felt, however, that these four tests are sufficient to establish the validity of the analysis given in Appendix B.

In Fig. 22, additional lines have been drawn to give a comparison of the theory here developed with other theories. If we adopt the analysis usually given in our text-books for hooks and eccentrically

loaded bars, in other words, if we neglect the curvature of the link, the theoretical line for the deflection of the minor axis is the line marked "ordinary theory." On the other hand, if we adopt Grashof's assumption (see page 6) we get the steep line marked "Grashof's theory."

The question of the probable distribution of pressure between adjacent links is not definitely settled. In most cases the experimental points follow most closely the line corresponding to case (a),

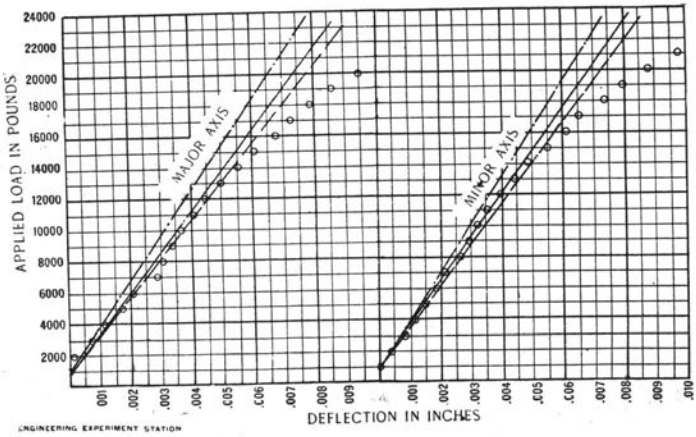

FIG. 23.

concentration at the end of the link, for the smaller loads. As the load is increased, however, the line through the points becomes steeper and its slope is about that of the theoretical line for case (b), distributed pressure. In a few of the experiments the points approached more closely the line for case (c). It is probable that the distribution depends somewhat upon the length of time a chain has been used. After the links have been fitted to each other and have worn slightly so as to make a bearing, the distribution will be that indicated by a line lying between the lines for cases (a) and (b). In this connection we may repeat the observation before made that in all cases the second test gave a line of greater slope than the first test.

By reference to Table 2 it will be seen that the assumed distribution influences in some measure the moment M at the end of the

minor axis, and through this the calculated stresses at various sections. The variation of M between cases (a) and (c) is about 7 per cent for the dredge link and 14 per cent for the conveyor link. If it is

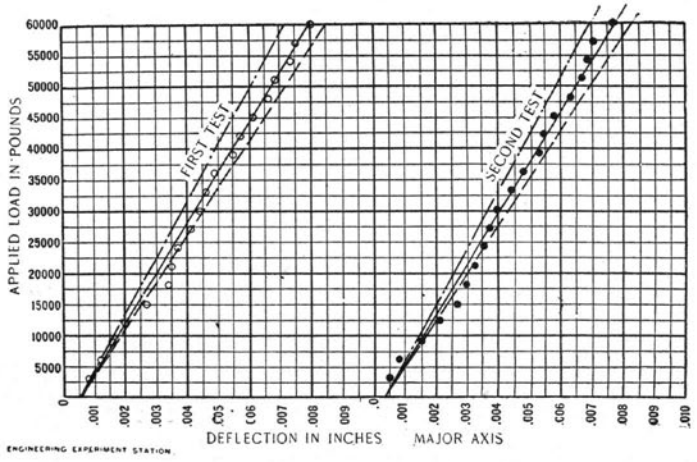

FIG. 24.

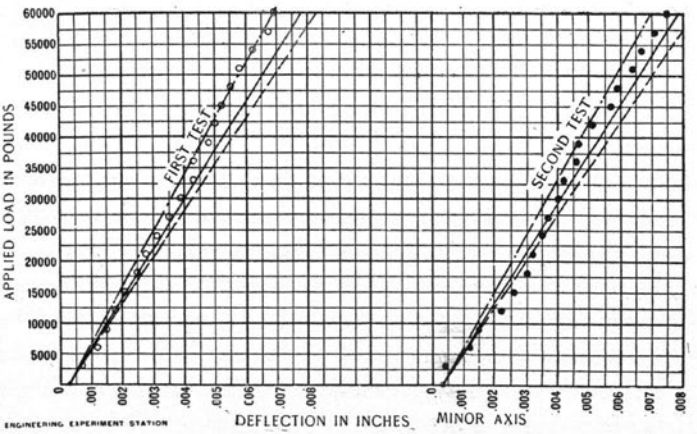

FIG. 25.

assumed that case (b) coincides most nearly with the actual distribution, the calculated stresses, taking the value of M from case (b), are not likely to vary more than 3 or 4 per cent from the actual

stresses even in the most extreme cases. Hence, in the subsequent calculations, we shall assume that the distribution is according to case (b).

Distribution of Stresses in Links

By means of the formulas developed in the Appendices, the intensity of stress can be calculated at any point of any cross section of the link. Thus for an open link, the moment M at the end of the short axis is found from formula (F), and from this the moment at any other section is readily obtained. Now having M_b and the normal force P at the section in question, the stress at different points in the section is found by using different values of y in formula (C). For the outer fiber $y = \frac{1}{2}d$, for the inner fiber $y = -\frac{1}{2}d$, at the axis $y = 0$, and so on.

These calculations have been made for the link shown in Fig. 5, and the results are exhibited in the following table:

TABLE 3

DISTRIBUTION OF STRESS IN OPEN LINK

ϕ	Normal Force P	Moment M_b	Stress at Center of Section $y=0$	Stress in Outer Fiber $y=+\frac{1}{2}d$	Stress in Inner Fiber $y=-\frac{1}{2}d$
0°	$0.225\,Q$	$+0.671\,Q$	$+0.896\,Q/f$	$+4.012\,Q/f$	$-8.453\,Q/f$
10°	0.257	+0.639	0.896	+3.863	−8.006
20°	0.352	+0.544	0.896	+3.420	−6.677
30°	0.500	+0.371	0.774	+2.785	−3.601
40°	0.643	+0.178	0.774	+1.739	−1.325
50°	0.766	+0.011	0.774	+0.836	+0.640
60°	0.866	−0.124	0.774	+0.104	+2.234
70°	0.940	−0.223	0.808	−0.504	+3.225
80°	0.985	−0.284	0.843	−0.917	+3.777
90°	1.000	−0.318	0.936	−1.366	+3.751
End of short axis	1.000	−0.318	1.000	−1.546	+3.546

A better idea of the distribution of stress through the link is shown in Fig. 26. At section a, lying along the minor axis, the inner fiber is subjected to a tensile stress of $3.55\frac{Q}{f}$, while the outer fiber is under a compression $1.55\frac{Q}{f}$. At section b, the tensile stress at the inner fiber

is a little greater, due entirely to the curvature at that section, and at section c this tensile stress is still greater because of the sharper curvature, notwithstanding the fact that the moment M_b is smaller. From here on, however, the tensile stress on the inside of the line rapidly decreases and reaches zero at the point L. At section e the moment M_b changes sign by passing through the value zero; hence at this section the stress is uniformly distributed and equal to $\frac{P}{f}$. From L to C the minor fiber of the link is in compression, the intensity of the compression reaching its maximum value $8.453\,\frac{Q}{f}$ at the point C. From A to K the outer fiber of the link is compressed, but from K to D it is in tension, the maximum intensity of the tension reaching the value $4.012\,\frac{Q}{f}$ at the point D. The lines HK and LM indicate the points of the link at which the stress is zero.

It will be observed that there are two points of maximum tensile stress; one at D, the other at E on the inside of the link. The compressive stress in the outer fibers is small; but at the point C it is very large.

The following table gives the stresses in the same link when provided with a stud; and Fig. 27 shows the distribution of stress in such a link.

TABLE 4

DISTRIBUTION OF STRESS IN STUD LINK

ϕ	Normal Force P	Moment M_b	Stress at Axis $y=0$	Stress in Outer Fiber $y=+\frac{1}{2}d$	Stress in Inner Fiber $y=-\frac{1}{2}d$
0°	$+0.555\,Q$	$+0.401\,Q$	$0.955\,Q/f$	$+2.814\,Q/f$	$-4.623\,Q/f$
10°	$+0.582$	$+0.373$	0.955	$+2.689$	-4.246
20°	$+0.662$	$+0.293$	0.955	$+2.314$	-3.123
30°	$+0.782$	$+0.152$	0.895	$+1.722$	-0.905
40°	$+0.892$	$+0.003$	0.895	$+0.913$	$+0.855$
50	$+0.975$	-0.109	0.895	$+0.304$	$+2.180$
60°	$+1.029$	-0.181	0.895	-0.089	$+3.034$
70°	$+1.051$	-0.211	0.895	-0.251	$+3.216$
80°	$+1.041$	-0.198	0.895	-0.180	$+3.186$
90°	$+1.000$	-0.056	0.989	$+0.587$	$+1.480$
End of short axis	$+1.000$	$+0.107$	1.000	$+1.858$	$+1.424$

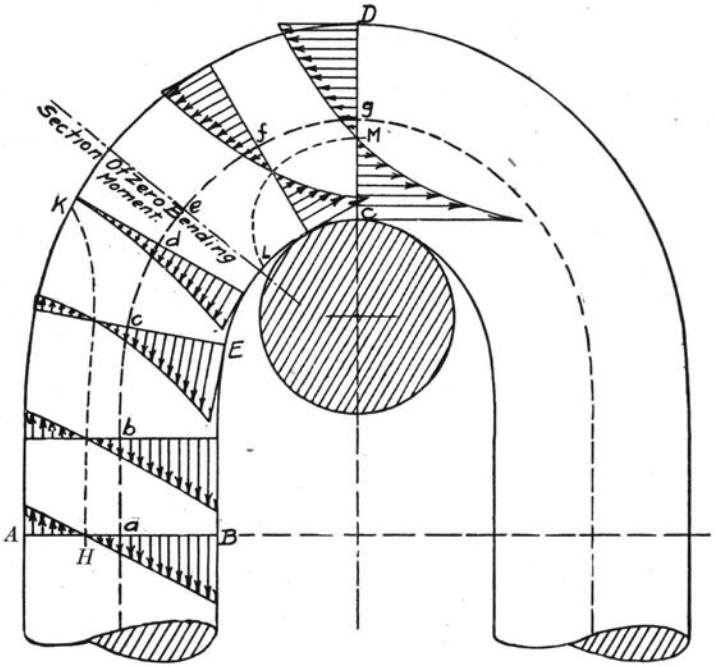
D
g
M
f
Section Of Zero Bending Moment.
K
e
d
C
E
c
b
A
a
H
B

FIG. 26.

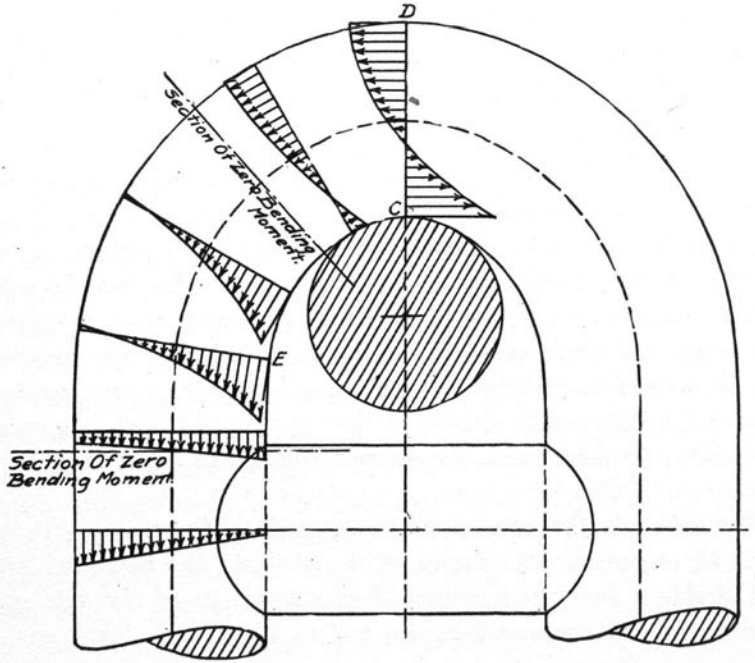
D
Section Of Zero Bending Moment.
C
E
Section Of zero Bending Moment.

FIG. 27.

It will be observed that in this case there are two sections at which the bending moment is zero. The tensile stress reaches a maximum for the outer fiber at D, and for the inner fiber at about the point E. The compression is greatest at point C, but is only a little over one-half that at C in the case of the open link. The tensile stresses are also somewhat smaller than for the open link.

The following table gives the maximum tensile stresses (at points D and E) and the maximum compressive stress (at point C) for each of the four links subjected to analysis.

TABLE 5

MAXIMUM STRESSES

Link	Open Link			Stud Link		
	Tensile Stress		Compressive Stress at C	Tensile Stress		Compressive Stress at C
	At E	At D		At E	At D	
Dredge, Fig. 3	3.98 Q/t	3.66 Q/t	8.38 Q/t	3.18 Q/t	2.81 Q/t	4.62 Q/t
Proof coil, Fig. 5	3.78	4.01	8.45	3.22	2.56	4.02
Two-inch, Fig. 6	3.72	3.47	7.94	3.20	2.38	3.54
Conveyor, Fig. 4	2.78	4.17	9.55	...	...	...

A study of the results presented in the preceding tables leads to some interesting conclusions:

In the first place, it may be observed that the maximum stresses for the different links are not widely different. The first three links may be regarded as typical of the forms ordinarily used in engineering practice, and in these the extreme variation in the maximum tensile stress is a little more than 7 per cent. It is also worthy of remark that the tensile stresses at the two points D and E are nearly the same. In some cases the greater stress will be at D, in others at E.

The conveyor link, on account of its relatively great length, presents an exception. As shown by the analysis, the increased length of the side makes the moment M at the middle of the side small; consequently the moment at the end of the link is large, and the

stress at D is considerably greater than that at E. It may be concluded, therefore, that so far as strength is concerned, the form of this link is not favorable.

The effect of the stud upon the distribution of stress is easily seen. The maximum tensile stresses are reduced about 20 per cent; but what is more essential, the heavy compressive stress at C is reduced 50 per cent or more. We conclude, therefore, that provided the stresses are kept within the elastic limit of the material, the stud is of unquestioned value.

It has been the general opinion of engineers that the stud link chain is stronger than the open link chain; however, the experiments of

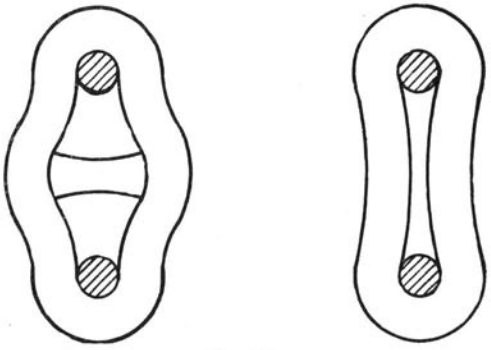

FIG. 28.

committee D of the United States board appointed to test iron. steel and other metals (see Executive Document No. 98, House of Representatives, Forty-fifth Congress, Second Session), seem to indicate that the stud actually weakens the chain, causing it to rupture at a load lower than that required to break an open link chain. At first sight these experiments seem to disprove the results given in the preceding pages; however, in this case, fact and theory are easily reconciled. It is quite easy to understand that while the stud link is much stronger than the open link, provided the elastic limit is not reached, the former may rupture with a smaller load than the latter. In the first place, the collapse of the sides of the open link after the elastic limit is passed decreases the effective width of the link, and thus decreases the bending moments and stresses. If the iron of

which the link is constructed is ductile, the link may collapse until the sides become nearly parallel, and the stresses are lower than in the stud link, the sides of which are prevented from collapsing by the stud. The appearance of the two forms of link under heavy load will be somewhat as shown in Fig. 28. Thus the actual distortion of the open link gives it a form of greater strength, which is not the case with the stud link.

Near the load producing rupture it seems likely, therefore, that the stresses in the open link are less than those in the stud link subjected to the same load. Within the elastic limit, however, the reverse is true, and there can be no doubt that for ordinary working loads the chain made of stud links is materially stronger than the one made of open links.

Formulas for the Loading of Chains

Unwin, *Elements of Machine Design*, Part I, p. 438, gives the following formulas:

$$P = 9\ d^2, \text{ for studded link chain;}$$
$$= 6\ d^2, \text{ for unstudded close link chain.}$$

He says further: "For much used chain, subject frequently to the maximum load, it is better to limit the stress to $3\frac{1}{4}$ tons per sq. in. Then

$$P = 5\ d^2."$$

In these formulas, P denotes the load in tons, and d the diameter in inches of the iron from which the chain is made.

Unwin says that Towne limits the loads in ordinary crane chains to

$$P = 3.3\ d^2,$$

but quotes the following table from Towne's *Treatise on Cranes*.

Diameter of Iron	$\frac{3}{16}$	$\frac{1}{4}$	$\frac{9}{32}$	$\frac{5}{16}$	$\frac{3}{8}$	$\frac{7}{16}$	$\frac{1}{2}$	$\frac{9}{16}$	$\frac{5}{8}$	$\frac{11}{16}$	$\frac{13}{16}$
Load on chain — tons	0.06	0.25	0.5	0.75	1	1.5	2	2.5	3	4	5

This table seems to be obtained from the formula

$$P = 8\,d^2.$$

Weisbach gives the formulas (Kent's *Pocket Book*, p. 339)

$$P = 17800\,d^2, \text{ stud link,}$$
$$P = 13350\,d^2, \text{ open link,}$$

where P denotes the load in pounds.

Bach, in his *Maschinenelemente*, p. 513, gives for chains with open links

$P = 1000\,d^2$ for new chains, maximum load seldom applied.
$P = 800\,d^2$ for much used chain.

P and d are taken in kilograms and centimeters, respectively. Using pounds and inches as the units, the formulas become

$$P = 13750\,d^2;$$
$$P = 11000\,d^2.$$

For a stud-link chain, Bach increases the safe load 20 per cent.

If we write the formula for the safe load

$$P = kd^2,$$

the values of k given by the authorities quoted are as follows, P being taken in pounds:

	Open Link	Stud Link
Unwin	13,440 11,200	20,160 ...
Weisbach	13,350	17,800
Bach	13,750 11,000	16,500 13,200

Referring to Table 5, we note that with links of the ordinary form the maximum tensile stresses are about as follows:

$$\left.\begin{array}{l} \text{for open links, } 4\,\dfrac{Q}{f}; \\ \text{for stud links, } 3.2\,\dfrac{Q}{f}. \end{array}\right\} \quad (1)$$

Of course these values will vary slightly with the form of the link; thus the conveyor link on account of its extreme length shows a maximum tensile stress of $4.17\frac{Q}{f}$. In general, however, the value $4\frac{Q}{f}$ cannot be very far from the truth for an open link of usual dimensions.

Denoting the load on the chain by P, and the maximum permissible unit stress by S, we have, since $P = 2Q$,

$$\left.\begin{aligned} &\text{for open links,} \quad S = \frac{4Q}{f} = \frac{2P}{f}; \\ &\text{for stud links,} \quad S = \frac{3.2Q}{f} = \frac{1.6P}{f}. \end{aligned}\right\} \tag{2}$$

Now taking $f = \frac{1}{4}\pi d^2$, we readily obtain

$$\left.\begin{aligned} &\text{for open links,} \quad P = \frac{1}{8}\pi d^2 S, \text{ say } 0.4\, d^2 S; \\ &\text{for stud links,} \quad P = \frac{1}{6.4}\pi d^2 S, \text{ say } 0.5 d^2 S. \end{aligned}\right\} \tag{3}$$

Comparing these equations with the equation

$$P = kd^2,$$

we see that

$$\left.\begin{aligned} k &= 0.4\, S, \quad \text{for open links,} \\ \text{and} \quad k &= 0.5\, S, \quad \text{for stud links.} \end{aligned}\right\} \tag{4}$$

Now using the values of k just given, we obtain the following values of S when we use the formulas ordinarily given.

	Open Link	Stud Link
Unwin	{ 33,600 { 28,000	...
Weisbach	33,375	40,320 35,600
Bach	{ 34,375 { 27,500	{ 33,000 { 26,400

It will probably be agreed that these values are considerably in excess of the values usually regarded as permissible in machine construction.

So far, we have considered only the tensile stresses. Referring to Table 5 it is seen that the compression at the end of the link is more than double the maximum tensile stress; hence when a chain has its full load, if the maximum tensile stress is 30,000 lb., as indicated by the constants above, the compressive stress at the end is something over 60,000 lb. It is probable that when the maximum load is applied, the pinching action heretofore described reduces to a considerable degree this excessive compression. Furthermore, it will be noted that the part of the link subjected to this compression is restrained laterally by the sides of the adjacent link; and this lateral restraint offsets in some measure the compressive stress. In any case, however, this compression is a factor to be seriously considered.

Using the maximum tensile stress as a basis, the formulas

$$P = 0.4\, d^2 S \text{ (open)} \tag{5}$$
$$P = 0.5\, d^2 S \text{ (stud)} \tag{6}$$

for open and stud links respectively, are proposed as substitutes for the formulas now in use. These formulas contain the safe maximum unit stress S, and are in that respect more general than those quoted from Unwin, Bach and others. If desired, the usual form $P = kd^2$ is readily obtained by assuming a proper value of S. Thus if S is taken at 15,000 lb. sq. in., we have

$$P = 6000\, d^2 \text{ (open)},$$
$$P = 7500\, d^2 \text{ (stud)},$$

respectively; if 20,000 lb. sq. in. is considered a permissible value of S, the formulas become

$$P = 8000\, d^2 \text{ (open)},$$
$$P = 10{,}000\, d^2 \text{ (stud)},$$

respectively.

Summary of Results, and Conclusions

The following is a summary of the results obtained from the investigations herein described and the conclusions that may be drawn from them:

1. The experiments on the steel rings confirm the theoretical analysis employed in the calculation of stresses.

2. The experiments on the various chain links further confirm the analysis and show that the distribution of pressure between the links, in general, lies between the extremes (*a*), point contact and (*c*), pressure concentrated at opposite points, as in Fig. 2(c). For purposes of calculation case (*b*), uniform distribution of pressure over an arc 2α may be assumed.

3. The load $2\,Q$ on the link produces an average intensity of stress $\frac{2\,Q}{2\,f} = \frac{Q}{f}$ in the cross section of the link containing the minor axis. With an open link of usual proportions the maximum tensile stress is approximately four times this value, i.e., $4\frac{Q}{f}$.

4. The introduction of a stud in the link equalizes the stresses throughout the link, reduces the maximum tensile stresses about 20 per cent, and reduces the excessive compressive stress at the end of the link about 50 per cent.

5. The stud-link chain of equal dimensions will, within the elastic limit, bear from 20 to 25 per cent more load than the open-link chain. The ultimate strength of the stud-link chain is, however, probably less than that of the open-link chain.

6. In the formulas for the safe loading of chains given by the leading authorities on machine design, the maximum stress to which the link is subjected seems to be underestimated and the constants are such as to give maximum stresses of from 30,000 to 40,000 lb. per sq. in. for full load.

7. The following formulas are applicable to chains of the usual form:

$$P = 0.4\,d^2S, \text{ for open links,}$$
$$P = 0.5\,d^2S, \text{ for stud links,}$$

where P denotes the safe load, d the diameter of the stock, and S the maximum permissible tensile stress.

TABLE 6

FIRST TEST OF 12-INCH STEEL RING NO. 1

Outside Diameter . . . . . 12.000 in.
Inside Diameter . . . . . 9.000 in.
Width . . . . . 1.0476 in.
Modulus of Elasticity 26,200,000

Applied Load Pounds	Extensometer Readings		Deformations	
	Horizontal Axis	Vertical Axis	Horizontal Axis	Vertical Axis
500	.2420	.2408	...	...
1,000	.2419	.2379	−.0001	.0029
1,500	.2442	.2367	.0022	.0041
2,020	.2467	.2357	.0047	.0051
2,500	.2474	.2342	.0054	.0066
3,000	.2484	.2322	.0064	.0086
3,500	.2494	.2306	.0074	.0102
4,000	.2503	.2277	.0083	.0131
4,500	.2529	.2284	.0109	.0124
5,000	.2536	.2270	.0116	.0138
5,500	.2546	.2256	.0126	.0152
5,900	.2550	.2249	.0130	.0159
6,500	.2572	.2234	.0152	.0174
7,000	.2583	.2218	.0163	.0190
7,500	.2600	.2187	.0180	.0221

TABLE 7

SECOND TEST OF 12-INCH STEEL RING NO. 1

Applied Load Pounds	Extensometer Readings		Deformations	
	Horizontal Axis	Vertical Axis	Horizontal Axis	Vertical Axis
0	.9985	.0024	...	...
500	.9975	.0048	.0012	.0024
1,000	.9960	.0045	.0025	.0021
1,500	.9948	.0057	.0036	.0033
2,000	.9933	.0073	.0052	.0049
2,500	.9917	.0085	.0068	.0061
3,000	.9913	.0098	.0072	.0074
3,500	.9907	.0116	.0078	.0092
4,000	.9890	.0130	.0095	.0106
4,500	.9874	.0143	.0111	.0119
5,000	.9863	.0156	.0122	.0132
5,500	.9851	.0170	.0134	.0146
6,000	.9840	.0184	.0145	.0160
6,500	.9824	.0199	.0161	.0175
7,000	.9808	.0213	.0177	.0189
7,500	.9800	.0223	.0185	.0199

TABLE 8

FIRST TEST OF STEEL RING NO. 2

Outside Diameter . . . . . 12.0056 in.
Inside Diameter . . . . . 9.000 in.
Thickness . . . . . 1.005 in.
Modulus of Elasticity 26,200,000

Applied Load Pounds	Extensometer Readings		Deformations	
	Horizontal Axis	Vertical Axis	Horizontal Axis	Vertical Axis
0	.0076	.0043	...	...
500	.0054	.0062	.0022	.0019
1,000	.0047	.0063	.0029	.0020
1,500	.0036	.0087	.0040	.0044
2,000	.0018	.0102	.0058	.0059
2,500	.0007	.0120	.0069	.0077
3,000	.9994	.0135	.0082	.0092
3,500	.9975	.0138	.0101	.0095
4,000	.9958	.0153	.0118	.0110
4,500	.9953	.0167	.0123	.0124
5,000	.9932	.0177	.0144	.0134
5,500	.9920	.0199	.0156	.0156
6,000	.9917	.0217	.0159	.0174
6,500	.9905	.0230	.0171	.0187
7,000	.9887	.0249	.0189	.0206
7,500	.9870	.0270	.0206	.0227

TABLE 9

SECOND TEST OF STEEL RING NO. 2

Applied Load Pounds	Extensometer Readings		Deformations	
	Horizontal Axis	Vertical Axis	Horizontal Axis	Vertical Axis
0	1.0050	.0062	....	...
500	1.0028	.0067	.0022	.0005
1,000	1.0023	.0082	.0027	.0020
1,500	1.0018	.0100	.0032	.0038
2,000	.9994	.0106	.0056	.0044
2,500	.9991	.0130	.0059	.0068
3,000	.9964	.0148	.0086	.0084
3,500	.9960	.0158	.0090	.0096
4,000	.9943	.0170	.0107	.0108
4,500	.9932	.0186	.0118	.0124
5,000	.9919	.0196	.0131	.0134
5,500	.9908	.0220	.0142	.0158
6,000	.9899	.0230	.0151	.0168
6,500	.9884	.0240	.0166	.0178
7,000	.9871	.0255	.0179	.0193
7,500	.9860	.0270	.0190	.0208

TABLE 10

FIRST TEST OF FORGED RING NO. 3

Outside Diameter . . . . . 12.007 in.
Inside Diameter . . . . . 9.001 in.
Width . . . . . 1.00 in.
Modulus of Elasticity 30,400,000

Applied Load Pounds	Extensometer Readings		Deformations	
	Horizontal Axis	Vertical Axis	Horizontal Axis	Vertical Axis
0	.0063	.0050	.0	.0
500	.0085	.0036	.0014	.0022
1,000	.0094	.0025	.0025	.0031
1,500	.0101	.0007	.0043	.0038
2,000	.0115	.9996	.0054	.0052
2,500	.0113	.9987	.0063	.0070
3,000	.0147	.9969	.0081	.0084
3,500	.0154	.9969	.0081	.0091
4,000	.0171	.9946	.0104	.0108
4,500	.0184	.9930	.0120	.0121
5,000	.0195	.9925	.0125	.0131
5,500	.0206	.9913	.0137	.0143
6,000	.0220	.9900	.0150	.0157
6,500	.0228	.9887	.0163	.0165
7,000	.0245	.9877	.0173	.0182
7,500	.0261	.9871	.0179	.0198
8,000	.0287	.9852	.0198	.0224

TABLE 11

SECOND TEST OF FORGED STEEL RING NO. 3

Applied Load	Extensometer Readings		Deformations	
	Horizontal Axis	Vertical Axis	Horizontal Axis	Vertical Axis
0	.0032	.0063	.0	.0
500	.0014	.0070	.0018	.0003
1,000	.0012	.0094	.0020	.0027
1,500	.0003	.0102	.0029	.0035
2,000	.9994	.0124	.0038	.0057
3,000	.9960	.0133	.0072	.0076
3,500	.9946	.0143	.0086	.0086
4,000	.9935	.0153	.0097	.0103
4,500	.9926	.0170	.0106	.0115
5,000	.9916	.0182	.0116	.0133
5,500	.9902	.0200	.0130	.0140
6,000	.9992	.0207	.0140	.0155
6,500	.9883	.0222	.0150	.0163
7,000	.9871	.0230	.0161	.0179
7,500	.9860	.0257	.0172	.0190
8,000	.9836	.0273	.0196	.0206

TABLE 12

FIRST TEST OF DREDGE LINK

Applied Load	Vertical Axis					Horizontal Axis	
	Readings		Differences		Deflections	Readings	Deflections
1,000	.0098	.0125	...	...	...	.5100	...
2,000	.0101	.0129	.0003	.0004	.00035	.5099	.0001
3,000	.0103	.0136	.0005	.0011	.0008	.5092	.0008
4,000	.0106	.0136	.0008	.0011	.00095	.5092	.0008
5,000	.0109	.0138	.0011	.0013	.0012	.5086	.0014
6,000	.0109	.0138	.0011	.0013	.0012	.5080	.0020
7,000	.0116	.0140	.0018	.0015	.00165	.5081	.0019
8,000	.0112	.0149	.0014	.0024	.0019	.5080	.0020
9,000	.0117	.0146	.0019	.0021	.0020	.5079	.0021
10,000	.0119	.0152	.0021	.0027	.0024	.5074	.0026
11,000	.0121	.0149	.0023	.0021	.0023	...	...
12,000	.0124	.0158	.0026	.0033	.00295	.5070	.0030
13,000	.0126	.0160	.0028	.0035	.00315	.5068	.0032
14,000	.0129	.0163	.0031	.0038	.00345	.5065	.0035
15,000	.0131	.0170	.0033	.0045	.0039	.5062	.0038
16,000	.0132	.0171	.0034	.0046	.0040	.5057	.0043
17,000	.0138	.0180	.0040	.0055	.00475	.5052	.0048
18,000	.0142	.0188	.0044	.0063	.00535	.5049	.0051
19,000	.0155	.0192	.0055	.0067	.0061	.5040	.0060
20,000	.0161	.0199	.0063	.0074	.00685	.5030	.0070
21,000	.0176	.0221	.0078	.0096	.0087	.5010	.0090
22,000	.0216	.0267	.0118	.0142	.0130	.4969	.0131

TABLE 13

SECOND TEST OF DREDGE LINK

[Modulus of Elasticity 24,600,000]

Applied Load	Vertical Axis					Horizontal Axis	
	Readings		Differences		Deflections	Readings	Deflections
1,000	.0033	.0035	...	...	...	.2036	...
2,000	.0035	.0038	.0002	.0003	.00025	.2035	.0001
4,000	.0038	.0045	.0005	.0010	.00075	.2034	.0002
6,000	.0042	.0054	.0009	.0019	.0014	.2030	.0006
8,000	.0048	.0062	.0015	.0027	.0021	.2024	.0012
10,000	.0048	.0072	.0015	.0037	.0026	.2016	.0020
12,000	.0051	.0078	.0018	.0043	.00305	.2013	.0023
14,000	.0059	.0085	.0028	.0050	.0038	.2010	.0026
16,000	.0061	.0088	.0025	.0053	.00405	.1999	.0037
18,000	.0058	.0101	.0028	.0066	.00455	.0997	.0039
20,000	.0068	.0111	.0033	.0076	.00545	.1990	.0046
22,000	.0069	.0120	.0036	.0085	.00695	.1981	.0055
24,000	.0326	.0248	.0293	.0213	.0253	...	...

TABLE 14

FIRST TEST OF CONVEYOR LINK

Applied Load	Vertical Axis					Horizontal Axis	
	Readings		Differences		Deflections	Readings	Deflections
1,500	.1363	.0400	...	...	...	.4875	...
2,000	.1368	.0399	.0005	.0001	.0002	.4880	.0005
2,500	.1371	.0407	.0008	.0007	.00075	.4870	.0005
3,000	.1383	.0401	.0020	.0001	.00105	.4869	.0006
3,500	.1389	.0401	.0026	.0001	.00135	.4865	.0010
4,000	.1390	.0404	.0027	.0004	.00155	.4863	.0012
4,500	.1495	.0407	.0032	.0007	.00195	.4860	.0015
5,000	.1398	.0408	.0035	.0008	.00215	.4860	.0015
5,500	.1401	.0409	.0038	.0009	.00235	.4855	.0020
6,000	.1401	.0416	.0038	.0016	.0027	.4853	.0022
6,500	.1404	.0410	.0041	.0010	.00255	.4850	.0025
7,000	.1405	.0412	.0042	.0012	.0027	.4847	.0028
7,500	.1408	.0413	.0045	.0013	.0029	.4843	.0032
8,000	.1410	.0417	.0047	.0017	.0032	.4840	.0038
8,500	.1411	.0418	.0048	.0018	.0033	.4837	.0038
9,000	.1413	.0419	.0050	.0019	.00345	.4834	.0041
9,000	.1408	.0422	...	...	...	.4832	...
10,000	.1420	.0425	.0062	.0022	.0042	.4830	.0043
11,000	.1425	.0429	.0067	.0026	.00465	.4822	.0053
12,000	.1427	.0430	.0069	.0027	.0048	.4814	.0061
13,000	.1432	.0436	.0074	.0033	.00535	.4810	.0065
14,000	.1434	.0443	.0076	.0040	.00580	.4800	.0075
15,000	.1437	.0448	.0079	.0045	.00620	.4791	.0084
16,000	.1443	.0452	.0085	.0049	.0067	.4782	.0093
17,000	.1448	.0459	.0090	.0056	.0073	.4774	.0101
18,000	.1458	.0459	.0100	.0056	.0078	.4766	.0109
19,000	.1462	.0463	.0104	.0060	.0082	.4754	.0121
20,000	.1470	.0470	.0112	.0067	.00895	.4740	.0135
21,000	.1485	.0474	.0127	.0071	.0099	.4724	.0151
22,000	.1499	.0480	.0141	.0077	.0109	.4710	.0165
23,000	.1517	.0498	.0159	.0095	.0127	...	...
24,000	.1533	.0512	.0175	.0109	.0142	.4660	.0215
25,000	.1569	.0551	.0211	.0148	.01795	.4620	.0255

TABLE 15

SECOND TEST OF CONVEYOR LINK

[Modulus of Elasticity, 28,400,000]

Applied Load	Vertical Axis					Horizontal Axis	
	Readings		Differences		Deflections	Reading	Deflections
1,120	.1835	.0292	...	...	...	.4013	...
2,040	.1840	.0295	.0005	.0003	.0004	.4010	.0003
3,020	.1843	.0300	.0008	.0008	.0008	.4003	.0010
4,000	.1848	.0302	.0013	.0010	.00115	.3996	.0017
5,110	.1852	.0308	.0017	.0016	.00165	.3984	.0029
6,040	.1858	.0312	.0023	.0020	.00215	.3981	.0032
7,000	.1860	.0315	.0025	.0023	.0024	.3978	.0035
8,030	.1864	.0319	.0029	.0027	.0028	.3969	.0044
9,190	.1867	.0323	.0032	.0031	.00315	.3964	.0049
10,000	.1873	.0326	.0038	.0034	.0036	.3960	.0053
11,000	.1880	.0329	.0045	.0037	.0041	.3956	.0057
12,020	.1882	.0332	.0047	.0040	.00435	.3949	.0064
13,090	.1886	.0336	.0051	.0044	.00475	.3942	.0071
14,090	.1890	.0341	.0055	.0049	.0052	.3936	.0077
15,030	.1892	.0345	.0057	.0053	.0055	.3930	.0083
16,090	.1895	.0347	.0060	.0055	.00575	.3924	.0089
17,020	.1897	.0350	.0062	.0058	.0060	.3920	.0093
18,000	.1898	.0356	.0063	.0064	.00635	.3914	.0099
19,000	.1907	.0355	.0072	.0063	.00675	.3910	.0103
20,000	.1910	.0359	.0075	.0067	.0071	.3904	.0109
21,000	.1918	.0365	.0083	.0073	.0078	.3899	.0114
22,000	.1922	.0367	.0087	.0075	.0081	.3893	.0120
23,000	.1923	.0372	.0088	.0080	.0084	.3884	.0129
24,000	.1928	.0378	.0093	.0086	.00895	.3878	.0135
25,000	.1933	.0380	.0098	.0088	.0093	.3873	.0140
26,000	.1940	.0382	.0105	.0090	.00975	.3870	.0143
27,000	.1944	.0389	.0109	.0097	.0103	.3860	.0153
28,000	.2081	.0562	.0246	.0270	.0258	...	...
29,000	.2185	.0673	.0350	.0381	.03655	...	...

TABLE 16

TEST OF PROOF COIL LINK

[Modulus of Elasticity, 26,100,000]

Applied Load	Vertical Axis					Horizontal Axis	
	Readings		Differences		Average Deflections	Readings	Deflections
1,000	.2006	.2002	...	...	...	.3872	...
2,000	.2010	.1006	.0004	.0004	.0004	.3870	.0002
3,000	.2017	.2008	.0011	.0006	.00085	.3864	.0008
4,000	.2021	.2010	.0015	.0008	.00115	.3860	.0012
5,000	.2022	.2016	.0016	.0014	.0015	.3854	.0018
6,000	.2026	.2019	.0020	.0017	.00185	.3851	.0021
7,000	.2030	.2021	.0024	.0019	.00215	.3843	.0029
8,000	.2034	.2027	.0028	.0025	.00265	.3841	.0031
9,000	.2038	.2929	.0032	.0027	.00295	.3838	.0034
10,000	.2041	.2032	.0035	.0030	.00325	.3835	.0037
11,000	.2045	.2034	.0039	.0032	.00355	.3831	.0041
12,000	.2049	.2038	.0043	.0036	.00395	.3827	.0045
13,000	.2054	.2043	.0048	.0041	.00445	.3822	.0050
14,000	.2060	.1047	.0052	.0045	.00485	.3816	.0056
15,000	.2066	.2052	.0060	.0050	.0055	.3811	.0061
16,000	.2071	.2059	.0065	.0057	.0061	.3804	.0068
17,000	.2078	.2061	.0072	.0059	.00655	.3799	.0073
18,000	.2087	.2068	.0081	.0066	.00735	.3793	.0079
19,000	.2097	.2070	.0091	.0068	.00795	.3786	.0086
20,000	.2108	.2076	.0102	.0074	.0088	.3777	.0095
21,000	.2119	.2088	.0113	.0086	.00975	.3763	.0109

TABLE 17

FIRST TEST OF TWO-INCH DREDGE LINK

[Modulus of Elasticity 29,000,000 (Assumed)]

Applied Load	Vertical Axis					Horizontal Axis	
	Readings		Differences		Deflections	Readings	Deflections
0	.0215	.5488	...	...	...	.5907	...
3,000	.0223	.5496	.0008	.0008	.0008	.5900	.0007
6,000	.0225	.5501	.0010	.0013	.0012	.5895	.0012
9,000	.0230	.5511	.0015	.0017	.0016	.5892	.0015
12,000	.0231	.5518	.0016	.0023	.0020	.5889	.0018
15,000	.0238	.5524	.0023	.0030	.0027	.5886	.0021
18,000	.0240	.5528	.0025	.0036	.0032	.5882	.0025
21,000	.0244	.5531	.0029	.0040	.0035	.5879	.0028
24,000	.0245	.5535	.0031	.0043	.0037	.5876	.0031
27,000	.0249	.5538	.0034	.0047	.0041	.5872	.0035
30,000	.0253	.5540	.0038	.0050	.0044	.5868	.0039
33,000	.0254	.5543	.0039	.0052	.0046	.5864	.0043
36,000	.0258	.5549	.0043	.0055	.0049	.5864	.0043
39,000	.0263	.5551	.0048	.0061	.0055	.5869	.0048
42,000	.0265	.5555	.0050	.0063	.0057	.5857	.0050
45,000	.0269	.5561	.0054	.0067	.0061	.5855	.0052
48,000	.0273	.5563	.0058	.0073	.0066	.5852	.0055
51,000	.0277	.5568	.0062	.0075	.0068	.5849	.0058
54,000	.0280	.5568	.0065	.0080	.0073	.5845	.0062
57,000	.0283	.5570	.0068	.0082	.0075	.5840	.0067
60,000	.0295	.5578	.0070	.0090	.0080	.5838	.0069

TABLE 18

SECOND TEST OF TWO-INCH DREDGE LINK

Applied Load	Vertical Axis					Horizontal Axis	
	Readings		Differences		Deflections	Readings	Deflections
0	.0216	.5495	...	...	...	.5902	...
3,000	.0219	.5502	.0003	.0007	.0005	.5898	.0004
6,000	.0223	.5505	.0007	.0010	.00085	.5890	.0012
9,000	.0228	.5514	.0012	.0019	.00155	.5887	.0015
12,000	.0230	.5523	.0014	.0028	.0021	.5880	.0022
15,000	.0235	.5530	.0019	.0035	.0027	.5876	.0026
18,000	.0238	.5532	.0022	.0037	.00295	.5872	.0030
21,000	.0241	.5535	.0025	.0040	.00325	.5870	.0032
24,000	.0242	.5540	.0026	.0045	.00355	.5867	.0035
27,000	.0246	.5540	.0030	.0045	.00375	.5865	.0037
30,000	.0247	.5543	.0031	.0048	.00395	.5862	.0040
33,000	.0251	.5548	.0035	.0053	.0044	.5860	.0042
36,000	.0255	.5552	.0039	.0057	.0048	.5856	.0046
39,000	.0259	.5558	.0043	.0063	.0053	.5855	.0047
42,000	.0260	.5560	.0044	.0065	.00545	.5851	.0051
45,000	.0265	.5562	.0049	.0067	.0058	.5845	.0057
48,000	.0270	.5568	.0054	.0073	.00635	.5843	.0059
51,000	.0275	.5570	.0059	.0075	.0067	.5838	.0064
54,000	.0278	.5571	.0062	.0076	.0069	.5838	.0067
60,000	.0280	.5573	.0064	.0078	.0071	.5831	.0071
75,000	.0285	.5580	.0068	.0085	.0077	.5827	.0075

TABLE OF SYMBOLS

Q = one-half of load applied to chain;

M_b = bending moment at any chosen section;

M = bending moment in side of link at end of minor axis;

P = normal force on any section of link;

s = intensity of stress at any point of a cross section;

ϕ = angle between any section and major axis of link;

α = one-half of assumed arc of contact between adjacent links;

f = area of cross section of link;

E = modulus of elasticity;

d = diameter of iron in link;

r = general symbol for radius of curvature;

r_2, r_3 = radii of curvature of parts of link;

ε = relative extension of any fiber;

ε_0 = relative extension of center line of link;

ω = ratio $\Delta d\phi : d\phi$;

y = distance of fiber from center line;

$z = -\frac{1}{f}\int \frac{y}{r+y}\, df$;

Δx, Δy = deflections of major and minor axes of link, respectively;

S = one-half of pressure between stud and side of link.

APPENDIX A

THEORY OF STRESSES IN CURVED BARS *

CONSIDER an element of the bar included between two cross sections A_1A_2 and C_1C_2, Fig. 29. The planes of these normal cross sections intersect in a line which pierces the plane of the paper at M; this line is the axis of curvature, that is, point M is the center of curvature

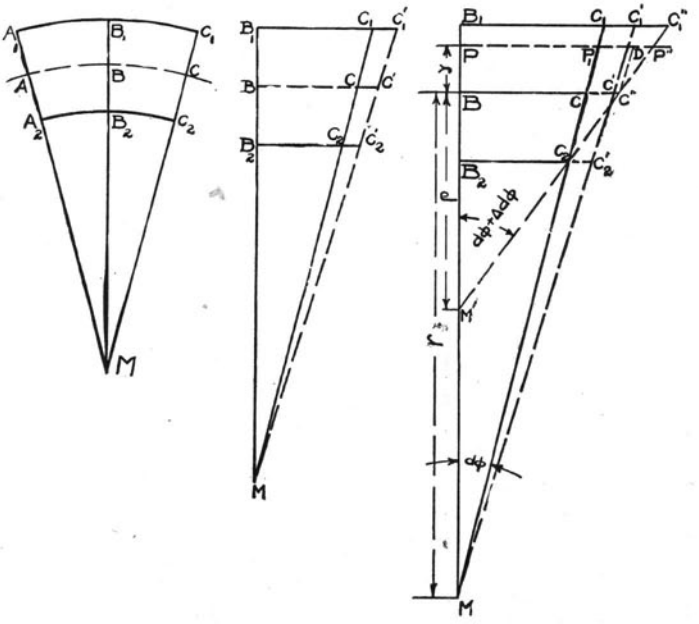

FIGS. 29, 30, 31.

of the center line AC. For the sake of convenience, we shall make use of only one-half of the element, as shown in Fig. 30, and we shall consider the sides B_1C_1, B_2C_2 to be straight lines, since the sections B_1B_2 and C_1C_2 are taken indefinitely close to each other.

* The theory here given is substantially that laid down by Bach, *Elasticitat und Festigkeit*, § 54.

Suppose now that an external force P acts at right angles to the section C_1C_2. If this force is uniformly distributed over the cross section C_1C_2, each fiber will be elongated (or shortened) by an amount proportional to its original length. Thus, assuming that the stress is tensile, we shall have

$$\frac{C_1C_1'}{B_1C_1} = \frac{CC'}{BC'} = \frac{C_2C_2'}{B_2C_2} = \text{a constant.}$$

It follows that the plane of the cross section will in its new position $C_1'C_2'$ pass through the axis of curvature M.

In addition to the force P normal to the section, let there be a couple of moment M_b acting at the section in question. It is assumed that the sense of the couple is such as to increase the curvature of the bar. The section C_1C_2 of the unloaded bar is brought to $C_1'C_2'$ by the normal force P, as just explained. The couple causes it to assume a new position $C_1''C_2''$, Fig. 31. The plane of the section in this position intersects the plane of the section B_1B_2 in the line M'. The angle between the cross sections is increased from $d\phi$ to $d\phi + \Delta d\phi$, and the radius of curvature is shortened from r to ρ.

Let ds denote the length BC and Δds the elongation CC'' due to the force P and moment M_b. The ratio $\dfrac{\Delta ds}{ds}$ we shall denote by ε_0;

hence
$$\varepsilon_0 = \frac{CC''}{BC}.$$

Consider now a fiber lying along PP_1 at a distance y from the center line BC. The extension of the fiber is P_1P''; hence we have

$$\varepsilon = \frac{P_1P''}{PP_1}.$$

To determine ε, let $C''D$ be drawn parallel to C_1C_2. Then

$$P_1P'' = P_1D + DP'' = CC'' + DP''$$
$$= \varepsilon_0 ds + y \cdot \text{angle } DC''P'' = \varepsilon_0 ds + y \cdot \Delta d\phi,$$

and
$$PP_1 = (y + r)d\phi.$$

Therefore
$$\varepsilon = \frac{\varepsilon_0 ds + y \cdot \Delta d\phi}{(r + y)\, d\phi} = \frac{\varepsilon_0 \dfrac{ds}{d\phi} + y \dfrac{\Delta d\phi}{d\phi}}{r + y}.$$

Let ω denote the ratio $\frac{\Delta d\phi}{d\phi}$; then since $ds = rd\phi$,

$$\varepsilon = \frac{\varepsilon_0 r + \omega y}{r + y} = \varepsilon_0 + (\omega - \varepsilon_0) \frac{y}{r + y} . \tag{1}$$

If E is the modulus of elasticity, the stress corresponding to the elongation ε is

$$s = E\varepsilon = E\left[\varepsilon_0 + (\omega - \varepsilon_0) \frac{y}{r + y}\right] . \tag{2}$$

The stresses developed over the section must hold in equilibrium the external forces and couples; hence denoting an element of the area of the section by df, we have from ordinary static conditions,

$$P = \int s\, df = \int E\left[\varepsilon_0 + (\omega - \varepsilon_0) \frac{y}{r + y}\right] df. \tag{3}$$

$$M_b = \int y \cdot s\, df = \int Ey\left[\varepsilon_0 + (\omega - \varepsilon_0) \frac{y}{r + y}\right] df. \tag{4}$$

The integrals involved, considering E a constant, are

$$\int df, \quad \int y\, df, \quad \int \frac{y}{r + y} df, \text{ and } \int \frac{y^2}{r + y} df.$$

Evidently $\int df = f$, and since y is measured from a gravity axis, $\int y df = 0$. For the sake of convenience, let

$$\int \frac{y}{r + y} df = - zf; \tag{5}$$

then

$$\int \frac{y^2}{r + y} df = \int \left(y - r \frac{y}{r + y}\right) df = - r \int \frac{y}{r + y} df = zfr. \tag{6}$$

Inserting these values of the integrals in (3) and (4), we get

$$P = Ef[\varepsilon_0 - (\omega - \varepsilon_0) z],$$
$$M_b = Ef(\omega - \varepsilon_0) zr.$$

By slight reduction the following important formulas are now obtained:

$$\omega \quad \varepsilon_0 = \frac{1}{Ef} \cdot \frac{M_b}{zr},$$

$$\varepsilon_0 = \frac{1}{Ef}\left(P + \frac{M_b}{r}\right), \tag{A}$$

$$\omega = \frac{1}{Ef}\left(P + \frac{M_b}{r} + \frac{M_b}{zr}\right). \tag{B}$$

Inserting the expressions for ε_0 and ω given by (A) and (B) in (2) we finally obtain for the intensity of stress at any point of the section

$$s = \frac{P}{f} + \frac{M_b}{fr} + \frac{M_b}{zfr} \cdot \frac{y}{r + y}. \tag{C}$$

Formula (C) gives the stress in terms of the force P, couple M_b, and other terms which depend solely upon the geometry of the system under consideration. In applying this formula care must be taken to give the quantities their proper signs. Thus:

P is positive when it tends to produce tension, negative when it tends to produce compression;

M_b is positive when it tends to increase the curvature of the bar, negative when it tends to decrease the curvature;

y is positive when measured towards the convex side of the bar, negative when measured towards the concave side, that is, towards the center of curvature.

When the value of s as determined from formula (C) is positive, the stress is tensile; if s is negative, the stress is compressive.

The function z as defined by (5), that is,

$$z = -\frac{1}{f} \int \frac{y}{r + y} df,$$

may be obtained by integration in the case of regular sections, circles, rectangles, etc. The following expressions for z are all that are required for present purposes.

For a circular cross section of radius a,

$$z = \frac{1}{4}\left(\frac{a}{r}\right)^2 + \frac{1}{8}\left(\frac{a}{r}\right)^4 + \frac{5}{64}\left(\frac{a}{r}\right)^6 + \frac{7}{128}\left(\frac{a}{r}\right) + \cdots$$

$$\frac{1}{z} = 4\left(\frac{r}{e}\right)^2 - 2 - \frac{1}{4}\left(\frac{e}{r}\right)^2 - \frac{1}{128}\left(\frac{e}{r}\right)^4 - \cdots$$

For a rectangular cross section of width b and depth $2a$,

$$z = \frac{1}{3}\left(\frac{a}{r}\right)^2 + \frac{1}{5}\left(\frac{a}{r}\right)^4 + \frac{1}{7}\left(\frac{a}{r}\right)^6 + \cdots$$

APPENDIX B

ANALYSIS OF OPEN LINK

To give an idea of the general method employed, a simple case is taken first, the more complicated general case later.

It is assumed that a quadrant of the center line of the link is made up of two circular arcs, Fig. 32, one, BE, having a radius equal to the

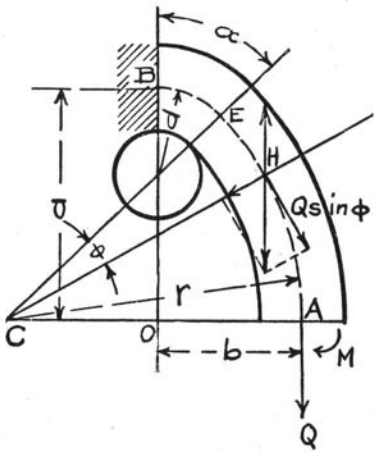

FIG. 32.

diameter d of the iron of the link, the other arc, EA, having a radius $AC = r$. Denoting by a and b the major and minor semi-axes, BO and AO, respectively, the following geometrical relations are easily deduced:

$$r = \frac{a^2 + b^2 - 2ad}{2(b - d)},$$

$$\sin \alpha = \frac{r - b}{r - d}, \quad \tan \alpha = \frac{r - b}{a - d}.$$

Let it be assumed first that the pressure between two links is concentrated at a point. Denoting this pressure by $2Q$, the normal

force at section A is Q. The unknown bending moment at this same section may be denoted by M. At any point H between E and A on the center line introduce two equal and opposite forces each equal to Q. One of these forces may be combined with Q giving a moment at H of magnitude

$$Qr\ (1 - \sin \phi).$$

Adding to this moment the moment M at section A, we have for the bending moment at section H,

$$M_b = M + Qr\ (1 - \sin \phi). \tag{1}$$

The other force at H may be resolved into two components, one normal to the section and thus producing tension, the other lying in the plane of the section. The latter component is neglected. The former has the value,

$$P = Q \sin \phi. \tag{2}$$

For sections lying between B and E, that is, for values of ϕ between 0 and α, we have likewise,

$$M_b = M + Q\ (b - d \sin \phi), \tag{3}$$
$$P = Q \sin \phi. \tag{4}$$

The unknown moment M is determined from the following considerations. As shown in Appendix A, the distortion of the link under load changes the angle $d\phi$ between two adjacent cross sections by the amount $\Delta d\phi$, this change being positive at some sections, negative at others. Because of the symmetry of the link, sections A and B originally at right angles remain at right angles; that is, the summation of the changes of angle $\Delta d\phi$ between B and A must be zero.

Hence
$$\sum_{B}^{A} \Delta d\phi = 0,$$

or since $\Delta d\phi = \omega \cdot d\phi$,

$$\int_0^{\alpha} \omega\, d\phi + \int_{\alpha}^{\frac{\pi}{2}} \omega\, d\phi = 0. \tag{5}$$

The general expression for ω [Eq. (B), Appendix A] is

$$\omega = \frac{1}{Ef}\left(P + \frac{M_b}{r} + \frac{M_b}{zr}\right). \tag{6}$$

For sections between $\phi = 0$ and $\phi = a$, $r = d$; hence,

$$\omega_1 = \frac{1}{Ef}\left(Q \sin \phi + \frac{M_b}{d} + \frac{M_b}{z_1 d}\right), \tag{7}$$

the subscript 1 being used to distinguish the ω and z of this part of the link from those of the other part. For sections lying between $\phi = \alpha$ and $\phi = \frac{\pi}{2}$,

$$\omega_2 = \frac{1}{Ef}\left(Q \sin \phi + \frac{M_b}{r} + \frac{M_b}{z_2 r}\right). \tag{8}$$

Inserting the proper values of the moment M_b from (1) and (3) we have,

$$\left.\begin{aligned} Ef\omega_1 &= \frac{M + Qb}{d}\left(1 + \frac{1}{z_1}\right) - \frac{Q}{z_1}\sin\phi, \\ Ef\omega_2 &= \frac{M + Qr}{r}\left(1 + \frac{1}{z_2}\right) - \frac{Q}{z_2}\sin\phi. \end{aligned}\right\} \tag{9}$$

Inserting these values of ω_1 and ω_2 in (5), integrating and reducing, we get finally,

$$M = Qd\left[\frac{\frac{1}{z_1}(1 - \cos\alpha) + \frac{1}{z_2}\cos\alpha - \alpha\frac{b}{d}\left(1 + \frac{1}{z_1}\right) - \left(1 + \frac{1}{z_2}\right)\left(\frac{\pi}{2} - \alpha\right)}{\alpha\left(1 + \frac{1}{z_1}\right) + \frac{d}{r}\left(1 + \frac{1}{z_2}\right)\left(\frac{\pi}{2} - \alpha\right)}\right] \tag{D}$$

The value of M being found by means of formula (D) the bending moment at any section is readily obtained; and with the bending

moment and normal force given, the intensity of stress at any fiber is readily determined by means of formula (C).

For a circular ring we have,

$$\left.\begin{aligned} P &= Q \sin \phi, \\ M_b &= M + Qr\,(1 - \sin \phi), \end{aligned}\right\} \tag{10}$$

whence $$\int_0^{\frac{\pi}{2}} \omega\, d\phi = \int_0^{\frac{\pi}{2}} \left[\left(\frac{M}{r} + Q\right)\left(1 + \frac{1}{z}\right) - \frac{Q \sin \phi}{z}\right] d\phi = 0.$$

Integrating and reducing,

$$M = Qr\left(\frac{2}{\pi\,(1 + z)} - 1\right). \tag{E}$$

We shall now take up a more complicated example which agrees more closely with conditions met in practice. In the first place, the

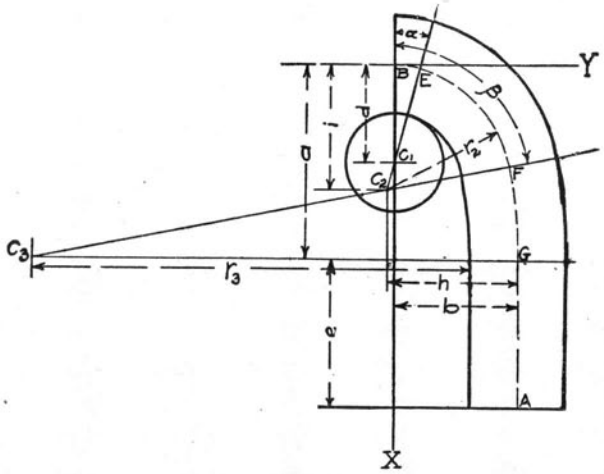

FIG. 33.

quadrant of the center line of the link cannot usually be represented closely by two circular arcs. Links actually measured show the form shown in Fig. 33. The center line BA is made up of four parts:

(1) the arc BE of radius d struck from C_1 as a center; (2) the arc EF with radius r_2 and C_2 as center; (3) the arc FG with radius r_3 and C_3 as center; (4) in some cases, a straight part of length e.

Secondly, as explained previously, the assumption that the pressure between adjacent links is concentrated at a point is not justified. We shall make the assumption that the pressure is distributed along an arc, as shown in Fig. 2 (b); afterwards the resulting equations will be modified to suit the assumption represented by Fig. 2 (c), namely that the pressure is regarded as concentrated at *two* points E and E.

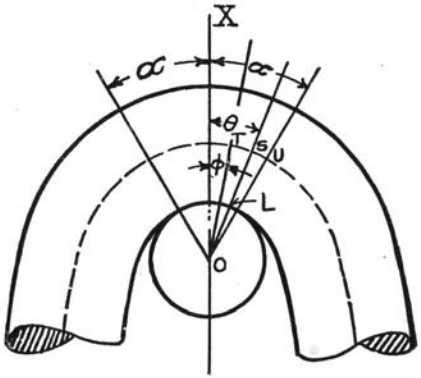

FIG. 34.

The distributed pressure along the angle of contact 2α (Fig. 34) gives rise to a normal force and a bending moment independent of the force Q and moment M at section A. We have now to derive expressions for the force P and moment M_b at any section included within the angle α.

The length of an element of arc of the circumference in contact is $\frac{d}{2}d\phi$; hence the pressure over the element of arc with the assumption of uniform distribution is

$$p\frac{d}{2}d\phi\,.$$

The vertical component of this force is

$$p\,\frac{d}{2}\cos\phi d\phi,$$

and the sum of such vertical components must be in equilibrium with the external force $2\,Q$. That is,

$$\frac{pd}{2}\int_{-\alpha}^{\alpha}\cos\phi\,d\phi = 2\,Q,$$

whence

$$pd\sin\alpha = 2\,Q,$$

or

$$p = \frac{2\,Q}{d\sin\alpha}.$$

Take any section OS making an angle θ with OX and for the present consider the angle ϕ constant. We are to find the moment and normal force at section T due to the distributed pressure between sections T and S. The intensity of pressure in the direction OS is p and the pressure along an element of arc of the circumference is therefore

$$dF = p\frac{d}{2}d\theta.$$

Now at T introduce two equal and opposite forces parallel to OS and of magnitude dF. One of these combines with dF acting through S to form a couple whose moment is,

$$d\sin(\theta-\phi)\,dF = p\,\frac{d^2}{2}\sin(\theta-\phi)\,d\theta.$$

The other force dF is resolved into components, the one perpendicular to section T being

$$p\frac{d}{2}\sin(\theta-\phi)\,d\theta.$$

If now we vary θ from ϕ to α and take the sum of the forces and moments for each element $d\theta$, we get:

$$\text{Normal force at } T = \frac{pd}{2}\int_{\phi}^{\alpha}\sin(\theta-\phi)\,d\theta;$$

$$\text{Moment at } T = \frac{pd^2}{2}\int_{\phi}^{\alpha}\sin(\theta-\phi)\,d\theta.$$

These are the force and moment at section T arising from the distributed pressure between sections T and U.
Taking ϕ constant, we obtain

$$\int_{\phi}^{\alpha} \sin(\theta - \phi)d\theta = 1 - \cos(\alpha - \phi),$$

and making use of the relation $p = \frac{2\theta}{d \sin \alpha}$ we get:

$$\text{Normal force at } T = \frac{Q}{\sin \alpha}[1 - \cos(\alpha - \phi)]; \tag{12}$$

$$\text{Moment at } T = \frac{Qd}{\sin \alpha}[1 - \cos(\alpha - \phi)]. \tag{13}$$

The normal force and moment at section T due to the force Q and moment M at section A have been shown to be respectively,

$$Q \sin \phi,$$

and

$$M + Q(b - d \sin \phi).$$

The total normal force at section T is therefore,

$$P = Q \sin \phi + \frac{Q}{\sin \alpha}[1 - \cos(\alpha - \phi)]$$

$$= \frac{Q}{\sin \alpha} - Q \cot \alpha \cos \phi. \tag{14}$$

The moment at T due to the distributed pressure is opposite in sense to the moment due to Q and M at section A; hence the net moment at T is

$$M_b = M + Qb - Qd \sin \phi - \frac{Qd}{\sin \alpha}[1 - \cos(\alpha - \phi)]$$

$$= M + Qb - \frac{Qd}{\sin \alpha} + Qd \cot \alpha \cos \phi. \tag{15}$$

Referring to Fig. 33, we see that (14) and (15) give the values of

P and M_b for cross sections lying between points B and E. Using these values we obtain for ω, the following expression:

$$\omega_1 = \frac{1}{Ef}\left[\frac{M + Qb}{\alpha}\left(1 + \frac{1}{z_1}\right) - \frac{Q}{z_1 \sin\alpha} + \frac{Q}{z_1}\cot\alpha\cos\phi\right]. \quad (16)$$

For the arc EF with radius r_2, the values of M_b and P are found to be,

$$\left.\begin{aligned} M_b &= M + Qh - Qr_2\sin\phi, \\ P &= Q\sin\phi, \end{aligned}\right\} \quad (17)$$

whence for this arc, ω_2 is given by the expression

$$\omega_2 = \frac{1}{Ef}\left[\frac{M + Qh}{r_2}\left(1 + \frac{1}{z_2}\right) - \frac{Q}{z_2}\sin\phi\right]. \quad (18)$$

For the arc FG, likewise

$$\left.\begin{aligned} M_b &= M + Qr_3 - Qr_3\sin\phi, \\ P &= Q\sin\phi, \end{aligned}\right\} \quad (19)$$

whence
$$\omega_3 = \frac{1}{Ef}\left[\frac{M + Qr_3}{r_3}\left(1 + \frac{1}{z_3}\right) - \frac{Q}{z_3}\sin\phi\right]. \quad (20)$$

For the straight part GA,

$$M_b = M, \qquad P = Q,$$

whence
$$\omega_4 = \frac{1}{Ef}\left[Q + \frac{M}{r_4}\left(1 + \frac{1}{z_4}\right)\right]. \quad (21)$$

Since the normal sections at B and A must remain at right angles, the summation of $\omega \cdot d\phi$ from B to A must be zero; that is

$$\int_0^\alpha \omega_1 d\phi + \int_\alpha^\beta \omega_2 d\phi + \int_\beta^{\frac{\pi}{2}} \omega_3 d\phi + \int_G^A \omega_4 d\phi = 0. \quad (22)$$

The first three integrals present no difficulties. Care must be taken in evaluating the last integral, however, because of the infinite factors that it contains. The expression for $\frac{1}{z_4}$ is

$$\frac{1}{z_4} = 16\left(\frac{r_4}{d}\right) - 2 - \frac{1}{16}\left(\frac{d}{r_4}\right) \cdots$$

Now since for the straight part GA, r_4 is infinite, it appears that $\frac{1}{z_4}$ is also infinite; and neglecting the finite terms, we may write (21) in the form

$$\omega_4 = \frac{1}{Ef} \cdot \frac{M}{r_4} \frac{16 r_4^2}{d^2} = \frac{16}{Ef} \frac{M r_4}{d^2}.$$

Therefore $$\omega_4 \, d\phi = \frac{16 \, M}{Efd^2} r_4 \, d\phi.$$

But $r_4 d\phi = ds$; hence

$$\int_G^A \omega_4 \, d\phi = \frac{16 \, M}{Efd^2} \int_0^e ds = \frac{1}{Ef} \cdot \frac{16 \, Me}{d^2}. \tag{23}$$

If now we substitute in (22) the values of ω_1, ω_2, and ω_3 given by (16), (18) and (20) and for the fourth integral the value just obtained we get the following (neglecting the constant factor Ef):

$$\frac{M + Qb}{d}\left(1 + \frac{1}{z_1}\right)\int_0^\alpha d\phi - \frac{Q}{z_1 \sin \alpha} \int_0^\alpha d\phi + \frac{Q}{z_1} \cot \alpha \int_0^\alpha \cos \phi \, d\phi$$

$$+ \frac{M + Qh}{r_2}\left(1 + \frac{1}{z_2}\right)\int_\alpha^\beta d\phi - \frac{Q}{z_2}\int_\alpha^\beta \sin \phi \, d\phi + \frac{M + Qr_3}{r_3}\left(1 + \frac{1}{z_3}\right)\int_\beta^{\frac{\pi}{2}} d\phi$$

$$- \frac{Q}{z_3}\int_\beta^{\frac{\pi}{2}} \sin \phi \, d\phi + 16 \frac{Me}{d^2} = 0.$$

Integrating and reducing, the following is obtained:

$$M = -Qd \left[\frac{\alpha \frac{b}{d}\left(1 + \frac{1}{z_1}\right) - \frac{1}{z}\left(\frac{\alpha}{\sin \alpha} - \cos \alpha\right) + \frac{h}{r_2}\left(1 + \frac{1}{z_2}\right)(\beta - \alpha) - \frac{1}{z_2}(\cos \alpha - \cos \beta) + \left(1 + \frac{1}{z_3}\right)\left(\frac{\pi}{2} - \beta\right) - \frac{\cos \beta}{z_3}}{\alpha\left(1 + \frac{1}{z_1}\right) + \frac{d}{r_2}\left(1 + \frac{1}{z_2}\right)(\beta - \alpha) + \frac{d}{r_3}\left(1 + \frac{1}{z_3}\right)\left(\frac{\pi}{2} - \beta\right) + 16 \frac{e}{d}} \right] \tag{F}$$

If the assumption is made that the pressure may be considered as concentrated at two points subtending the angle 2α (see Fig. 2 (c)), we readily obtain instead of (12) and (13):

$$\text{Normal force at } T = Q \sec \alpha \sin (\alpha - \phi). \tag{12'}$$

$$\text{Moment at } T = Qd \sec \alpha \sin (\alpha - \phi). \tag{13'}$$

Equations (14) and (15) then become

$$P = Q \tan \alpha \cos \phi, \tag{14'}$$

$$M_b = M + Qb - Qd \tan \alpha \cos \phi, \tag{15'}$$

whence

$$\omega_1 = \frac{1}{Ef}\left[\frac{M + Qb}{d}\left(1 + \frac{1}{z_1}\right) - \frac{Q}{z_1} \tan \alpha \cos \phi\right]. \tag{16'}$$

Using this value of ω_1 in (22), we get finally

$$M = -Qd\left[\frac{\alpha\frac{b}{d}\left(1+\frac{1}{z_1}\right)-\frac{1}{z_1}\tan\alpha\sin\alpha+\frac{h}{r_2}\left(1+\frac{1}{z_2}\right)\left(\beta-\alpha\right) - \frac{1}{z_2}\left(\cos\alpha-\cos\beta\right)+\left(1+\frac{1}{z_3}\right)\left(\frac{\pi}{2}-\beta\right)-\frac{\cos\beta}{z_3}}{\alpha\left(1+\frac{1}{z_1}\right)+\frac{d}{r_2}\left(1+\frac{1}{z_2}\right)(\beta-\alpha)+\frac{d}{r_3}\left(1+\frac{1}{z_3}\right)\left(\frac{\pi}{2}-\beta\right)+16\frac{e}{d}}\right] \tag{F'}$$

It will be observed that the change in the assumed law of distribution changes the second term in the numerator of (F) from

$$\frac{1}{z_1}\left(\frac{\alpha}{\sin \alpha} - \cos \alpha\right) \quad \text{to} \quad \frac{1}{z_1} \tan \alpha \sin \alpha.$$

If we assume concentration at the end of the link this term is

$$\frac{1}{z_1}(1 - \cos \alpha).$$

From the value of M as determined from (F) or (F'), the bending moment M_b at any section is obtained, and then the stress at any fiber is found by means of (C).

APPENDIX C

DERIVATION OF THEORETICAL FORMULAS FOR THE CHANGE OF LENGTH IN THE AXES OF THE LINK

THE analysis given in Appendices A and B may be employed to calculate the change in length of either axis of the link due to a given load. As has been stated, the comparison of this calculated change of length with the change actually measured is the basis of the experimental verification of the theory.

The following discussion is substantially that given by Bach: Let $O\ P\ C\ D$, Fig. 35, be the center line of a curved bar before it is

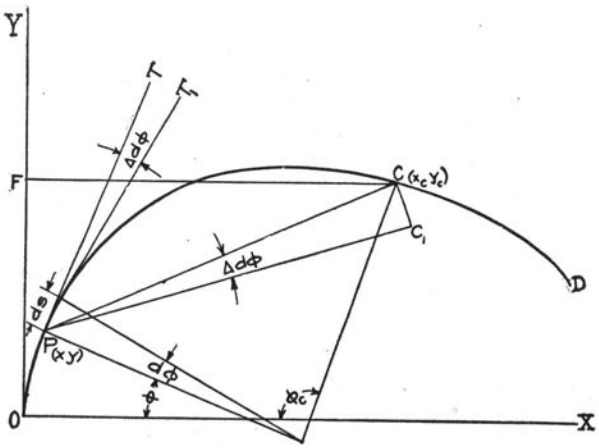

FIG. 35.

subjected to external forces. The point O is chosen as the origin, and the tangent and normal at O are taken as the Y- and X-axes respectively. When the bar is subjected to external forces, it is distorted and the center line changes its form. Any point C is thereby moved to a new position, and if x_c, y_c are the original coördinates

of C, these receive increments Δx_c and Δy_c respectively. These increments we now propose to determine by the principles hitherto developed.

Choose any point P whose coördinates are x, y, and let r be the radius of curvature at this point. An element of arc at P has the direction PT and its length is $ds = rd\phi$, where ϕ as usual denotes the angle between r and the x-axis. Because of the action of the external forces and couples, this element of arc will turn about P — which we for the present consider fixed — through the angle $\Delta d\phi$. This rotation causes the point C to move to C_1 on the circular arc $CC_1 = PC \cdot \Delta d\phi$. The components of the displacement CC_1 along the X- and Y-axes are respectively

$$\left.\begin{aligned} &PC \cdot \Delta d\phi \sin PCF = \quad PC \cdot \sin PCF \cdot \Delta d\phi = (y_c - y) \cdot \Delta d\phi \\ \text{and} \\ &-PC \cdot \Delta d\phi \cos PCF = -PC \cdot \cos PCF \cdot \Delta d\phi = -(x_c - x) \cdot \Delta d\phi \end{aligned}\right\} \quad (1)$$

In addition to the coördinate increments due to the change in inclination of the section at P there are increments due to the lengthening (or shortening) of the arc element ds at P. The extension of the element is $\varepsilon_0 ds$; hence because of this extension the point C is moved in the direction of the X-axis a distance,

$$\varepsilon_0 ds \sin \phi = \varepsilon_0 dx$$

and in the direction of the Y-axis a distance

$$\varepsilon_0 ds \cos \phi = \varepsilon_0 dy.$$

Adding together the changes just deduced (and replacing $\Delta d\phi$ by $\omega \cdot d\phi$), we have:

$$\left.\begin{aligned} &\text{change along } X\text{-axis} = (y_c - y)\, \omega d\phi + \varepsilon_0 dx, \\ &\text{change along } Y\text{-axis} = -(x_c - x)\, \omega d\phi + \varepsilon_0 dy. \end{aligned}\right\} \quad (2)$$

The total increments of the coördinates x_c and y_c, made up of the changes for all the arc elements lying between O and C, are found by summation. Thus,

$$\left.\begin{aligned} \Delta x_c &= y_c \int_0^{\phi_c} \omega\, d\phi - \int_0^{\phi_c} y\alpha\, d\phi + \int_0^{x_c} \varepsilon_0 dx, \\ \Delta y_c &= \int_0^{\phi_c} x\omega\, d\phi - x_c \int_0^{\phi_c} \omega\, d\phi + \int_0^{y_c} \varepsilon_0 dy. \end{aligned}\right\} \quad (G)$$

We have now to apply these fundamental formulas (a) to the circular ring and (b) to the chain link.

I. *Distortion of Circular Ring*

Referring to Fig. 36, it is evident that the point A at the extremity of the transverse diameter is the point whose coördinate increments

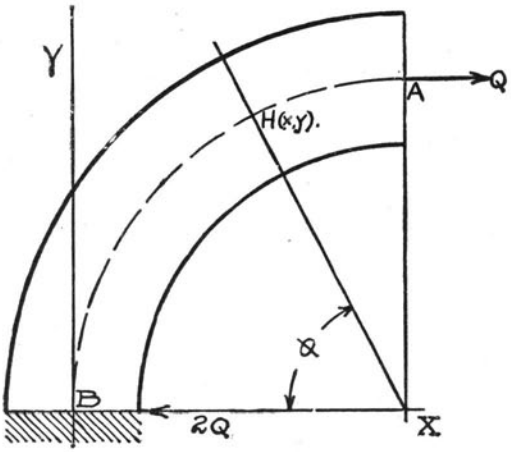

FIG. 36.

are desired. Denoting by x, y the coördinates of any point H on the center line between A and B, we have

$$\left.\begin{aligned} x_a &= y_a = r, \\ x_a - x &= r\cos\phi, \\ y &= r\sin\phi. \end{aligned}\right\} \tag{3}$$

At H, the normal force and bending moment are

$$\left.\begin{aligned} P &= Q\sin\phi, \\ M_b &= M + Qr\,(1 - \sin\phi), \end{aligned}\right\} \tag{4}$$

whence

$$Ef\cdot\varepsilon_0 = \frac{M + Qr}{r}, \tag{5}$$

and

$$Ef\cdot\omega = \frac{M + Qr}{r}\left(1 + \frac{1}{z}\right) - \frac{Q\sin\phi}{z}. \tag{6}$$

Since for the quadrant BA, $\int \omega \, d\phi = 0$, the first of equations (G) reduces to the simpler form

$$\Delta x_a = -\int_0^{\frac{\pi}{2}} y\omega \, d\phi + \int_0^r \varepsilon_0 \, dx. \tag{7}$$

Inserting in (7) proper values from (3), (5) and (6), we get,

$$Ef \cdot \Delta x_a = -(M + Qr)\left(1 + \frac{1}{z}\right)\int_0^{\frac{\pi}{2}} \sin\phi \, d\phi + \frac{Qr}{z}\int_0^{\frac{\pi}{2}} \sin^2\phi \, d\phi + \frac{M + Qr}{r}\int_0^r dx.$$

$$= -(M + Qr)\left(1 + \frac{1}{z}\right) + \frac{Qr\pi}{4z} + M + Qr$$

$$= -\frac{1}{z}(M + Qr) + \frac{\pi}{4}\frac{Qr}{z}.$$

In a similar way,

$$\Delta y_a = -\int_0^{\frac{\pi}{2}} (x_a - x)\omega \cdot d\phi + \int_0^r \varepsilon_0 \, dy = -\int_0^{\frac{\pi}{2}} r\cos\phi \cdot \omega \, d\phi + \int_0^r \varepsilon_0 dy.$$

$$Ef \cdot \Delta y_a = -(M + Qr)\left(1 + \frac{1}{z}\right)\int_0^{\frac{\pi}{2}} \cos\phi \, d\phi + \frac{Qr}{z}\int_0^{\frac{\pi}{2}} \sin\phi\cos\phi \, d\phi + \frac{M + Qr}{r}\int_0^r dy$$

$$= -\frac{1}{z}(M + Qr) + \frac{Qr}{2z}.$$

These results may be written as follows:

$$\left.\begin{aligned} \Delta x_a &= -\frac{1}{Ef} \cdot \frac{1}{z}\left[M + Qr\left(1 - \frac{\pi}{4}\right)\right], \\ \Delta y_a &= -\frac{1}{Ef} \cdot \frac{1}{z}\left[M + \tfrac{1}{2} Qr\right]. \end{aligned}\right\} \tag{H}$$

If finally the expression for M given by equation (E) be introduced, the equations take the form

$$\left.\begin{aligned}\Delta x_a &= -\frac{1}{Ef}\cdot\frac{Qr}{z}\left[\frac{2}{\pi\,(1+z)}-\frac{\pi}{4}\right],\\ \Delta y_a &= -\frac{1}{Ef}\cdot\frac{Qr}{z}\left[\frac{2}{\pi\,(1+z)}-0.5\right].\end{aligned}\right\} \qquad (H')$$

II. *Distortion of Chain Link*

Referring to Fig. 33, the point A at the end of the minor axis is the point whose movement under load is desired. Since for the quadrant BA, $\int \omega\, d\phi = 0$, the equations (G) when applied to the coördinates of point A become simply,

$$\left.\begin{aligned}\Delta x_a &= -\int_0^{\phi_a} y\omega\, d\phi + \int_0^{x_a}\varepsilon_0\, dx,\\ \Delta y_a &= \int_0^{\phi_a} x\omega\, d\phi + \int_0^{y_a}\varepsilon_0\, dy.\end{aligned}\right\} \qquad (G')$$

There are four parts in the quadrant BA of the center line; hence separate expressions for x, y, ω and ε_0 must be derived for each of these parts and furthermore the integrations must be separated.

From the geometry of Fig. 33, and from the results obtained previously (Appendix B) we have the following:

For arc BE, subtending angle α

$$\left\{\begin{aligned} x &= d(1-\cos\phi),\quad y = d\sin\phi.\\ P &= \frac{Q}{\sin\alpha} - Q\cot\alpha\cos\phi.\\ M_b &= M + Qb - \frac{Q\,d}{\sin\alpha} + Qd\cot\alpha\cos\phi.\\ Ef\cdot\varepsilon_0 &= \frac{M+Qb}{d}.\\ Ef\cdot\omega &= \frac{M+Qb}{d}\left(1+\frac{1}{z_1}\right) - \frac{Q}{z_1}\left(\frac{1}{\sin\alpha}+\cot\alpha\cos\phi\right).\end{aligned}\right.$$

For arc EF, subtending angle $\beta - \alpha$

$$x = i - r_2 \cos\phi, \quad y = r_2 \sin\phi + b - h.$$
$$P = Q \sin\phi.$$
$$M_b = M + Qh - Qr_2 \sin\phi.$$
$$Ef \cdot \varepsilon_0 = \frac{M + Qh}{r_2}.$$
$$Ef \cdot \omega = \frac{M + Qh}{r_2}\left(1 + \frac{1}{z_2}\right) - \frac{Q}{z_2} \sin\phi.$$

For arc FG, subtending angle $\frac{\pi}{2} - \beta$

$$x = a - r_3 \cos\phi, \quad y_3 = b - r_3 + r_3 \sin\phi.$$
$$P = Q \sin\phi.$$
$$M_b = M + Qr_3 - Qr_3 \sin\phi.$$
$$Ef \cdot \varepsilon_0 = \frac{M + Qr_3}{r_3}.$$
$$Ef \cdot \omega = \frac{M + Qr_3}{r_3}\left(1 + \frac{1}{z_3}\right) - \frac{Q}{z_3} \sin\alpha.$$

For straight part GA

$$x = a + u, \quad y = b.$$
$$P = Q.$$
$$M_b = M.$$
$$Ef \cdot \varepsilon_0 = Q.$$
$$Ef \cdot \omega = 16\, M \frac{r_4}{d^2}.$$

The above expressions for x, y, ε_0 and ω are substituted in the equations (G′) and the resulting integrals are evaluated for each arc separately. Then the results are combined.

For the straight part GA, the radius r_4 is infinite, and care must be exercised to get correct results. Letting u denote the distance of a point in GA from G, we have

$$x = a + u,$$

whence

$$x\omega\, d\phi = 16 \frac{M}{d^2} (a + u)\, r_4 d\phi.$$

But

$$r_4 d\phi = du,$$

and therefore

$$\int x\omega\, d\phi = \frac{16\,M}{d^2}\int_0 (a+u)\, du = 16\frac{M}{d^2}\left(ae+\frac{e^2}{2}\right).$$

Likewise $\int y\omega\, d\phi = \frac{16\,Mb}{d^2}\int_0 du = 16\,\frac{Mbe}{d^2}$.

It is readily seen that for the part GA,

$$\int \varepsilon_0 dx = Qe, \text{ and } \int \varepsilon_0 dy = 0.$$

The results of the substitution and integration are the following equations:

$$\begin{aligned}
Ef\,.\,\Delta x_a = &-\frac{1}{z_1}(1-\cos\alpha)\,(M+Qb)-\frac{Qd}{2z_1}\left[\frac{2\,(1-\cos\alpha)}{\sin\alpha}-\sin\alpha\cos\alpha\right]\\
&-\frac{1}{z_2}(\cos\alpha-\cos\beta)\,(M+Qh)\\
&+\frac{Qr_2}{2z_2}\,[\beta-\alpha+\sin\alpha\cos\alpha-\sin\beta\cos\beta]\\
&+\frac{h-b}{r_2}\left(1+\frac{1}{z_2}\right)(\beta-\alpha)\,(M+Qh)\\
&-\frac{1}{z_2}(\cos\alpha-\cos\beta)\,(h-b)\,Q-\frac{\cos\beta}{z_3}(M+Qr_3)\\
&+\frac{Qr_3}{2z_3}\left(\frac{\pi}{2}-\beta+\sin\beta\cos\beta\right)\\
&+\left(1+\frac{1}{z_3}\right)\left(\frac{r_3-b}{r_3}\right)\left(\frac{\pi}{2}-\beta\right)(M+Qr_3)\\
&-(r_3-b)\,\frac{\cos\beta}{z_3}\,Q+Qe-\frac{16\,be}{d^2}\,M. \qquad \textbf{(J)}\\
Ef\,.\,\Delta y_a = &\;\alpha\left(1+\frac{1}{z_1}\right)(M+Qb)+\frac{Qd}{z_1}(1+\cos\alpha)\\
&-\frac{Qd}{2z_1}\left(\frac{2\,\alpha-\alpha\cos\alpha}{\sin\alpha}+\cos^2\alpha\right)\\
&-\frac{1}{z_1}\sin\alpha\,(M+Qb)+\frac{i}{r_2}\left(1+\frac{1}{z_2}\right)(\beta-\alpha)\,(M+Qh)\\
&-\frac{1}{z_2}(\sin\beta-\sin\alpha)\,(M+Qh)
\end{aligned}$$

$$-\frac{Qi}{z_2}(\cos\alpha - \cos\beta) + \frac{Qr_2}{2z_2}(\sin^2\beta - \sin^2\alpha)$$
$$+\frac{a}{r_3}\left(1+\frac{1}{z_3}\right)\left(\frac{\pi}{2}-\beta\right)(M + Qr_3)$$
$$-\frac{1}{z_3}(1 - \sin\beta)(M + Qr_3) - \frac{Qa\cos\beta}{z_3} + \frac{Qr_3}{2z_3}(1 - \sin^2\beta)$$
$$+\frac{16M}{d^2}\left(me + \frac{e^2}{2}\right). \qquad \text{(K)}$$

It will be observed that both (J) and (K) have the general form,

$$Ef \cdot \Delta = c_1 M + c_2 Q \qquad (8)$$

where c_1 and c_2 are constants depending entirely upon the dimensions and configuration of the link. Since however,

$$M = kQ$$

we have $$\Delta x_a = c'Q, \quad \Delta y_a = c''Q \qquad (9)$$

where c' and c'' are other constants. Equation (9) shows that the change in the length of either axis is directly proportional to the load.

APPENDIX D

ANALYSIS OF STUD-LINK.

When the link has a transverse stud, as shown in Fig. 37, the analysis of the stresses is much more complicated than in the case of the open link. Hence we shall give here only the general method of attack and the final equations.

Referring to Fig. 37, let $2S$ denote the pressure between the end of the stud and the side of the link. Then one-half of this pressure may

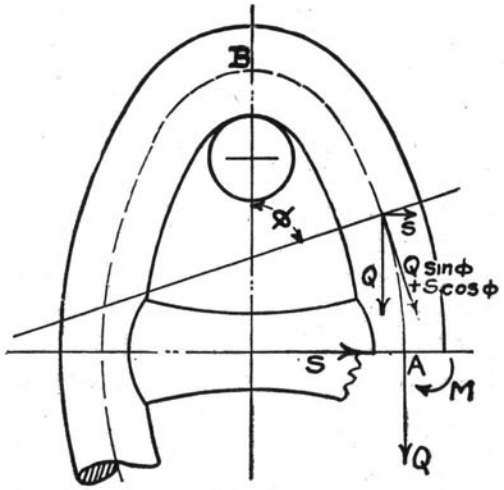

Fig. 37.

be considered as acting on the quadrant AB of the link; and to simplify the work, we shall assume the line of action of this force S to lie in the minor axis of the link. The quadrant AB is therefore subjected to the external force Q and moment M, as before, and in addition to the transverse force S.

The introduction of this force S gives rise to new terms in the expressions for the normal force and bending moment at any section.

Assuming the link quadrant to be made up of three circular arcs and a straight part, as shown in Fig. 33, we readily obtain the following results:

For arc BE,

$$\begin{cases} P = \dfrac{Q}{\sin\alpha} - Q\cot\alpha\cos\phi + S\cos\phi, \\ M_b = M + Qb - \dfrac{Qd}{\sin\alpha} + Qd\cot\alpha\cos\phi - S(a + e - d + d\cos\phi). \end{cases}$$

For arc EF,
$$\begin{cases} P = Q\sin\phi + S\cos\phi, \\ M_b = M + Qh - Qr_2\sin\phi - S(a + e - i + r_2\cos\phi). \end{cases}$$

For arc FG,
$$\begin{cases} P = Q\sin\phi + S\cos\phi, \\ M_b = M + Qr_3 - Qr_3\sin\phi - S(e + r_3\cos\phi). \end{cases}$$

For straight part GA,
$$\begin{cases} P = Q, \\ M_b = M - S(e - u). \end{cases}$$

From these expressions for P and M_b we may derive expressions for ε_0 and ω as in Appendix C for open links.

We have in the case of the stud link two unknown quantities to determine, the force S and the moment M at the section A; hence we must obtain two relations between M, S, and Q. As in the analysis of the open link, one equation is found from the relation

$$\int_{\text{Sec. } B}^{\text{Sec. } A} \omega \cdot d\phi = 0. \tag{1}$$

To obtain a second relation, we make use of the fact that the decrease in the length of the minor axis must be equal to the decrease in the length of the stud. Now an expression for the change of the minor axis may be found by the method of Appendix C, using equations (G′). The length of the stud may be taken as $2b - d$; hence if E' and f' denote respectively the modulus of elasticity of the material of the stud and the average area of cross-section, we have

$$\text{decrease of length} = \frac{2S(2b - d)}{E'f'}. \tag{2}$$

One-half of this decrease of length is equal to Δy_a the change of the Y- coördinate of the point A of the link. We have therefore,

$$-\Delta y_a = \frac{S\,(2b-d)}{E'f'}. \tag{3}$$

If now we denote by k the ratio $\frac{Ef}{E'f'}$ we obtain finally

$$-Ef\,.\,\Delta y_a = kS\,(2b-d). \tag{4}$$

Equation (4) gives a second relation between M, S and Q. The following simultaneous equations are finally obtained:

$$\left.\begin{aligned} A_1M &= B_1Sd - C_1Qd, \\ A_2M &= B_2Sd - C_2Qd, \end{aligned}\right\} \tag{5}$$

in which the coefficients have the following values:

$$A_1 = \alpha\left(1+\frac{1}{z_1}\right)+\frac{d}{r_2}\left(1+\frac{1}{z_2}\right)(\beta-\alpha)+\frac{d}{r_3}\left(1+\frac{1}{z_3}\right)\left(\frac{\pi}{2}-\beta\right)+16\frac{e}{d}.$$

$$B_1 = \alpha\left(1+\frac{1}{z_1}\right)\frac{a+e-d}{d}+\frac{1}{z_1}\sin\alpha+\left(1+\frac{1}{z_2}\right)\left(\frac{a+e-i}{r_2}\right)(\beta-\alpha)$$
$$+\frac{1}{z_2}(\sin\beta-\sin\alpha)$$
$$+\frac{e}{r_3}\left(1+\frac{1}{z_3}\right)\left(\frac{\pi}{2}-\beta\right)+\frac{1}{z_3}(1-\sin\beta)+8\frac{e^2}{d^2}.$$

$$C_1 = \alpha\frac{b}{d}\left(1+\frac{1}{z_1}\right)+\frac{h}{r_2}\left(1+\frac{1}{z_2}\right)(\beta-\alpha)+\left(1+\frac{1}{z_3}\right)\left(\frac{\pi}{2}-\beta\right)$$
$$-\frac{1}{z_1}\left(\frac{\alpha}{\sin\alpha}-\cos\alpha\right)-\frac{1}{z_2}\cos\alpha-\cos\beta)-\frac{1}{z_3}\cos\beta.$$

$$A_2 = \alpha\left(1+\frac{1}{z_1}\right)-\frac{1}{z_1}\sin\alpha+\frac{i}{r_2}\left(1+\frac{1}{z_2}\right)\left(\beta-\alpha\right)-\frac{1}{z_2}(\sin\beta-\sin\alpha)$$
$$-\frac{1}{z_3}(1-\sin\beta)$$
$$+\frac{a}{r_3}\left(1+\frac{1}{z_3}\right)\left(\frac{\pi}{2}-\beta\right)+8\left(\frac{2ae+e^2}{d^2}\right).$$

$$B_2 = \alpha\left(1+\frac{1}{z_1}\right)\frac{a+e-d}{d}-\frac{1}{z_1}\left(\frac{a+e-2d}{d}\right)\sin\alpha$$
$$-\frac{1}{2z_1}(d+\sin\alpha\cos\alpha)$$

$$+\frac{i}{r_2}\left(\frac{a+e-i}{d}\right)\left(1+\frac{1}{z_2}\right)(\beta-d)-\frac{1}{z_2}\left(\frac{a+e-2i}{d}\right)(\sin\beta-\sin\alpha)$$

$$-\frac{1}{2z_2}\frac{r_2}{d}(\beta-\alpha+\sin\beta\cos\beta-\sin\alpha\cos\alpha)$$

$$+\frac{1}{z_3}\left(\frac{a-e}{d}\right)(1-\sin\beta)+\frac{ae}{r_3 d}\left(1+\frac{1}{z_3}\right)\left(\frac{\pi}{2}-\beta\right)$$

$$-\frac{1}{2z_3}\frac{r_3}{d}\left(\frac{\pi}{2}-\beta-\sin\beta\cos\beta\right)+\frac{8}{3}\frac{e^2}{d^3}(3a+e)-k\left(\frac{2b-d}{d}\right).$$

$$C_2=\alpha\frac{b}{d}\left(1+\frac{1}{z_1}\right)-\frac{1}{z_1}\left(\frac{\alpha}{\sin\alpha}-\cos\alpha\right)-\frac{1}{z_1}\left(\frac{b}{d}\sin\alpha-1\right)$$

$$-\frac{1}{2z_1}(\alpha\cot\alpha+\cos^2\alpha)+\frac{ih}{r_2 d}\left(1+\frac{1}{z_2}\right)(\beta-\alpha)$$

$$-\frac{1}{z_2}\frac{i}{d}(\cos\alpha-\cos\beta)-\frac{1}{z_2}\frac{h}{d}(\sin\beta-\sin\alpha)$$

$$+\frac{1}{2z_2}\frac{r_2}{d}(\sin^2\beta-\sin^2\alpha)+\frac{a}{d}\left(1+\frac{1}{z_3}\right)\left(\frac{\pi}{2}-\beta\right)-\frac{1}{z_3}\frac{a}{d}\cos\beta$$

$$-\frac{1}{z_3}\frac{r_3}{d}(1-\sin\beta)+\frac{1}{2z_3}\frac{r_3}{d}(1-\sin^2\beta).$$

These coefficients are first determined from the known constants z_1, z_2, and z_3, and the known dimensions of the link. The solution of Eqs. (5) then gives the values of M and S, and from these, values of the normal force P and moment M_b for any section are readily found. Having P and M_b, the stress at any point of the cross section is found from the general equation (C).

With the open link the greatest tensile stress is either at the end or at the side of the link, that is, at sections on the major or minor axis. See Fig. 26. In the case of the stud link, the greatest tensile stress is usually at a point on the inside of the link at some distance from the end of the minor axis. See Fig. 27. To determine the exact position of the section of maximum tension, we insert the expressions for P and M_b in (C) and thus obtain

$$S = c + m\,(Q\sin\phi + S\cos\phi),$$

in which c and m are constant for all sections.

Taking the first derivative, we get,

$$\frac{dS}{d\phi} = m\,(Q\cos\phi - S\sin\phi),$$

and equating this to zero, we find

$$\frac{Q}{S} = \tan\phi.$$

Hence at the section for which

$$\phi = \tan^{-1}\frac{Q}{S},$$

the tensile stress will be a maximum.

PUBLICATIONS OF THE ENGINEERING EXPERIMENT STATION

Bulletin No. 1. Tests of Reinforced Concrete Beams, by Arthur N. Talbot. 1904. (*Out of print*).

Circular No. 1. High-Speed Tool Steels, by L. P. Breckenridge. 1905.

Bulletin No. 2. Tests of High-Speed Tool Steels on Cast Iron, by L. P. Breckenridge and Henry B. Dirks. 1905.

Circular No. 2. Drainage of Earth Roads, by Ira O. Baker. 1906.

Bulletin No. 3. The Engineering Experiment Station of the University of Illinois, by L. P. Breckenridge. 1906. (*Out of print*).

Bulletin No. 4. Tests of Reinforced Concrete Beams, Series of 1905, by Arthur N. Talbot. 1906.

Bulletin No. 5. Resistance of Tubes to Collapse, by Albert P. Carman. 1906. (*Out of print*).

Bulletin No. 6. Holding Power of Railroad Spikes, by Roy I. Webber. 1906.

Bulletin No. 7. Fuel Tests with Illinois Coals, by L. P. Breckenridge, S. W. Parr and Henry B. Dirks. 1906.

Bulletin No. 8. Tests of Concrete: I. Shear; II. Bond, by Arthur N. Talbot. 1906. (*Out of print*).

Bulletin No. 9. An Extension of the Dewey Decimal System of Classification Applied to the Engineering Industries, by L. P. Breckenridge and G. A. Goodenough. 1906.

Bulletin No. 10. Tests of Plain and Reinforced Concrete Columns, Series of 1906, by Arthur N. Talbot. 1907.

Bulletin No. 11. The Effect of Scale on the Transmission of Heat through Locomotive Boiler Tubes, by Edward C. Schmidt and John M. Snodgrass. 1907. (*Out of print*).

Bulletin No. 12. Tests of Reinforced Concrete T-Beams, Series of 1906, by Arthur N. Talbot. 1907.

Bulletin No. 13. An Extension of the Dewey Decimal System of Classification Applied to Architecture and Building, by N. Clifford Ricker. 1907.

Bulletin No. 14. Tests of Reinforced Concrete Beams, Series of 1906, by Arthur N. Talbot. 1907.

Bulletin No. 15. How to Burn Illinois Coal without Smoke, by L. P. Breckenridge. 1908.

Bulletin No. 16. A Study of Roof Trusses, by N. Clifford Ricker. 1908.

Bulletin No. 17. The Weathering of Coal, by S. W. Parr, N. D. Hamilton and W. F. Wheeler. 1908.

Bulletin No. 18. The Strength of Chain Links, by G. A. Goodenough, and L E. Moore. 1908.

Bulletin No. 19. Comparative Tests of Carbon, Metallized Carbon and Tantalum Filament Lamps by T. H. Amrine. 1908.